From a Different Angle: A Little Creativity Can Help

Jim Connell
University of New Hampshire
Department of Physics & Astronomy
and
Space Science Center

High Energy Charged Particles in Space (> few MeV)

1. Particles accelerated at planetary magnetospheres
2. Solar energetic particles (SEPs) are accelerated by events on the Sun or by phenomena originating on the Sun
3. Anomalous cosmic rays (ACRs) are local interstellar material accelerated in the Heliosphere
4. Galactic cosmic rays (GCRs) enter the Solar system from the Galaxy (and beyond!)

In order of increasing scale: planets, Sun, Heliosphere, Galaxy
Also in order of increasing maximum energy.

Scintillating Optical Fiber Isotope Experiment (SOFIE)

Figure 2.3

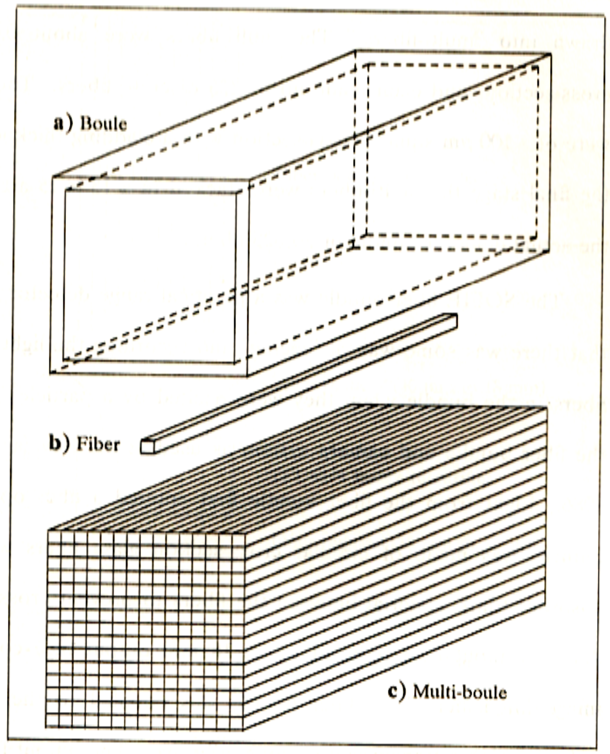

Diagram showing: a) cladded boule of square cross–section; b) fiber, also of square cross–section; c) multi–fiber boule made from square fibers. Figure not to scale.

Some considerable Skepticism

ACE/CRIS

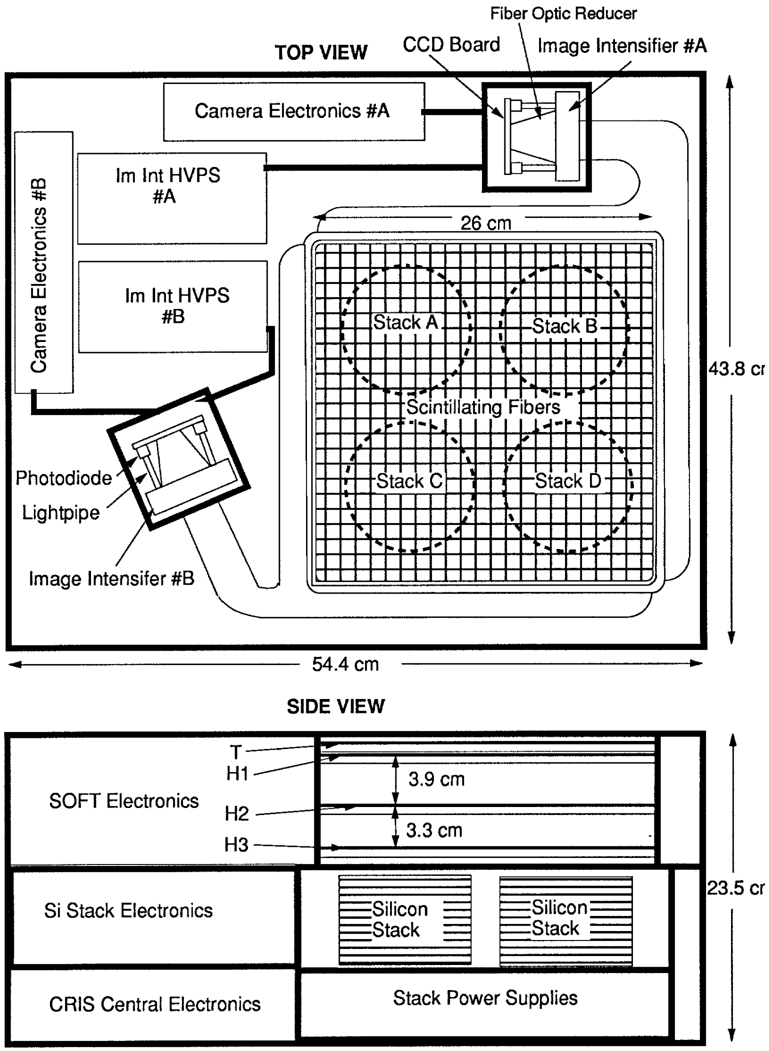
TOP VIEW
Fiber Optic Reducer
CCD Board
Image Intensifier #A
Camera Electronics #A
Im Int HVPS #A
Im Int HVPS #B
Camera Electronics #B
26 cm
Stack A
Stack B
Scintillating Fibers
Stack C
Stack D
43.8 cm
Photodiode
Lightpipe
Image Intensifer #B
54.4 cm
SIDE VIEW
T
H1
3.9 cm
SOFT Electronics
H2
3.3 cm
H3
Si Stack Electronics
Silicon Stack
Silicon Stack
23.5 cm
CRIS Central Electronics
Stack Power Supplies

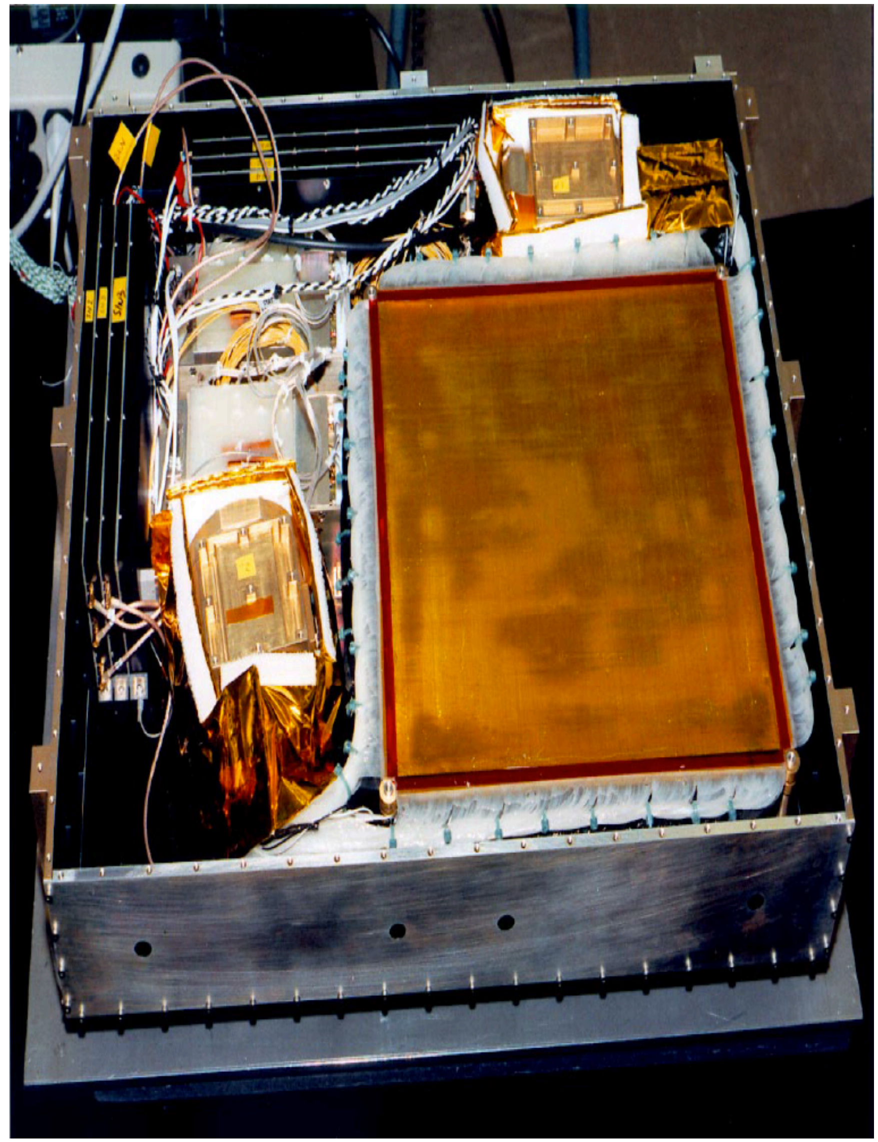

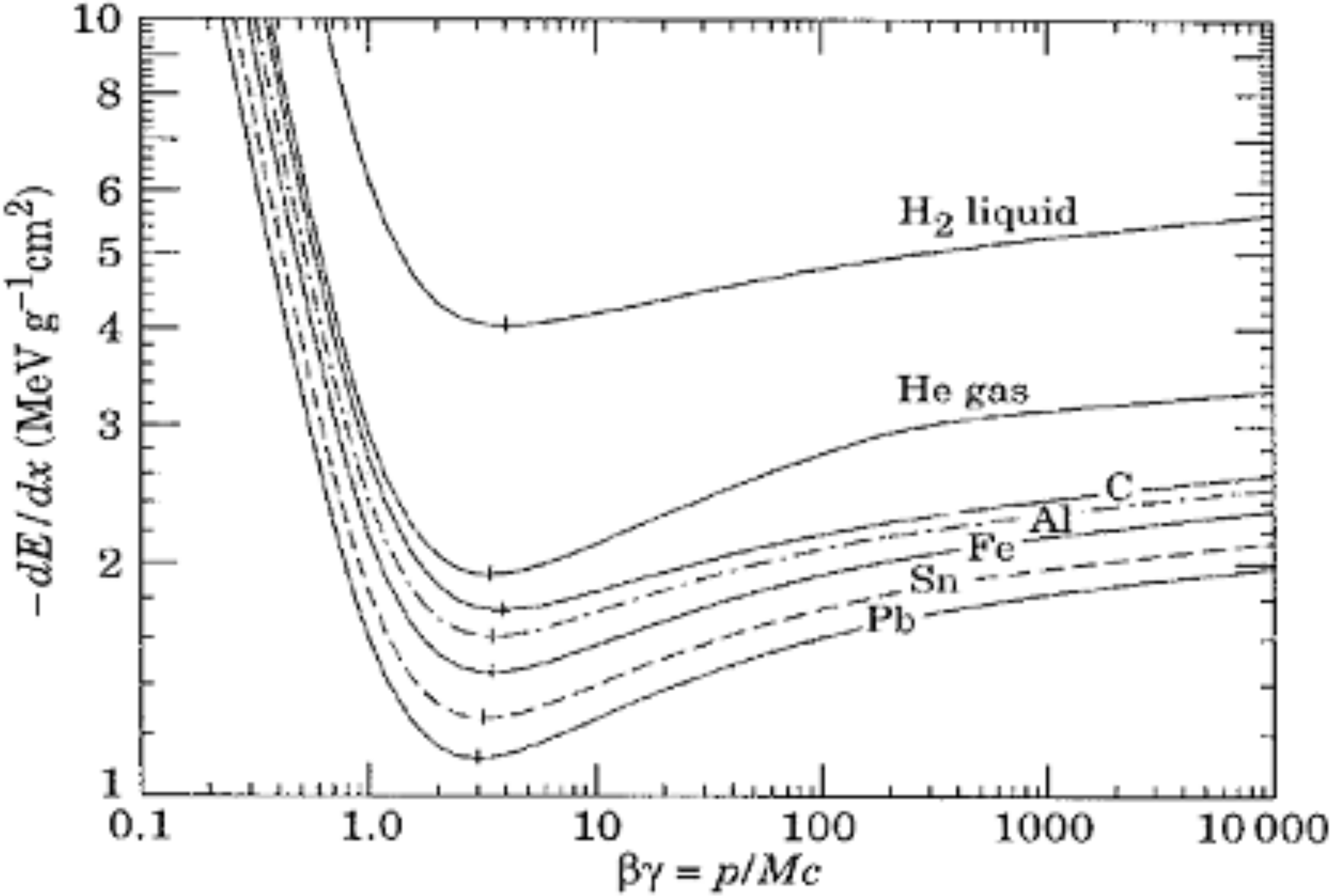

10
8
6
5
4
3
2
1
$-dE/dx$ (MeV $g^{-1}cm^2$)
H_2 liquid
He gas
C
Al
Fe
Sn
Pb
0.1
1.0
10
100
1000
10 000
$\beta\gamma = p/Mc$

Bethe-Bloch Formula

$$\Delta p = F\Delta t \sim \frac{Ze^2}{4\pi\varepsilon_0 g^2}\frac{1}{\beta c}$$

Bethe-Bloch Formula

$$\Delta p = F\Delta t \sim \frac{Ze^2}{4\pi\varepsilon_0 g^2}\frac{1}{\beta c}$$

$$\Delta E = \frac{(\Delta p)^2}{2m_e} \sim \frac{Z^2 e^4}{32\pi^2\varepsilon_0^2 m_e c^2 \beta^2}\frac{1}{g^4}$$

Bethe-Bloch Formula

$$\Delta p = F\Delta t \sim \frac{Ze^2}{4\pi\varepsilon_0 g^2}\frac{1}{\beta c}$$

$$\Delta E = \frac{(\Delta p)^2}{2m_e} \sim \frac{Z^2e^4}{32\pi^2\varepsilon_0^2 m_e c^2\beta^2}\frac{1}{g^4}$$

$$-\frac{dE}{dx} = \frac{Z^2e^4N_e}{4\pi\varepsilon_0^2 m_e c^2\beta^2}\left[\ln\left(\frac{2\gamma m_e c^2\beta^2}{I_{adj}}\right) - \beta^2\right]$$

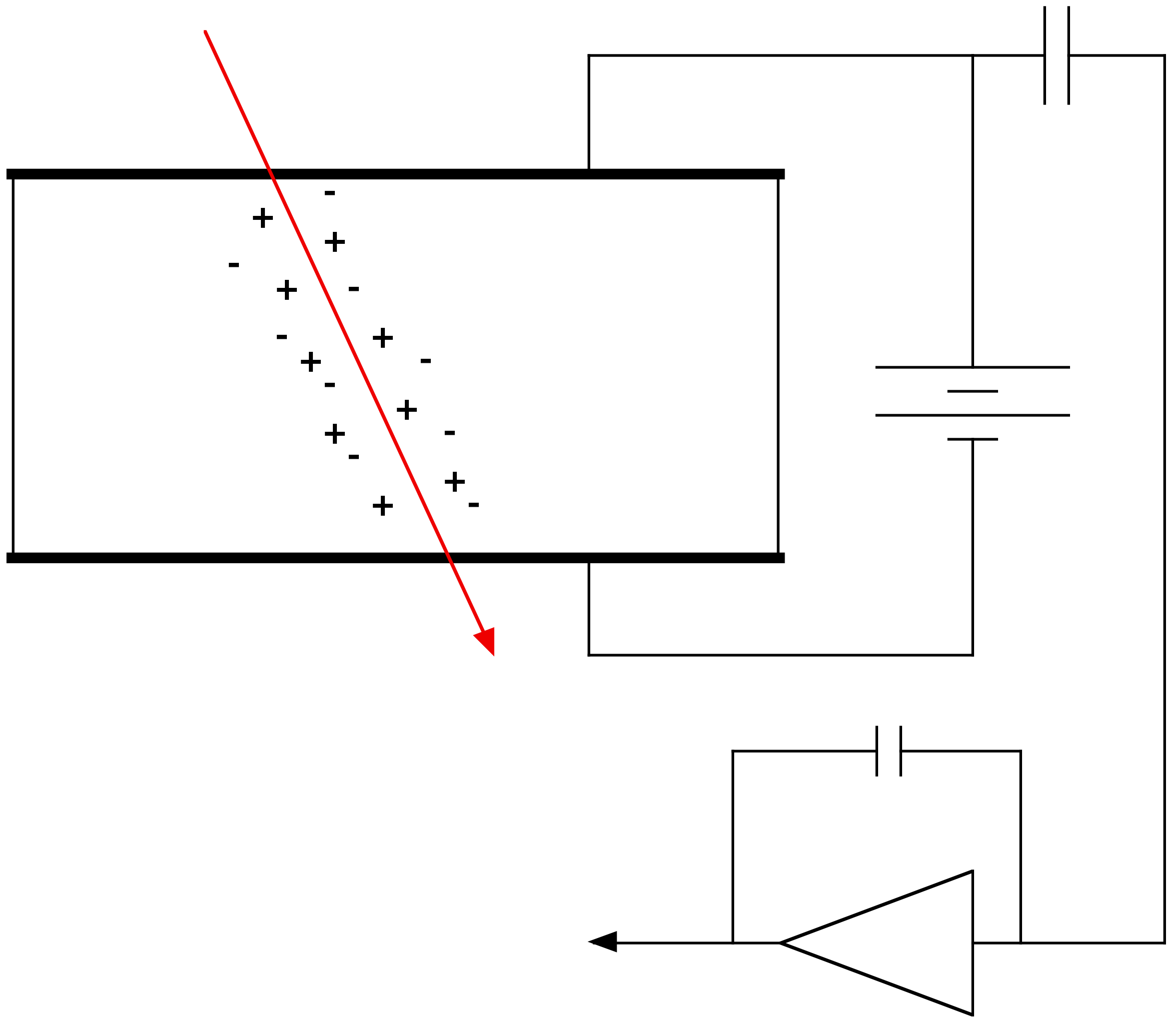

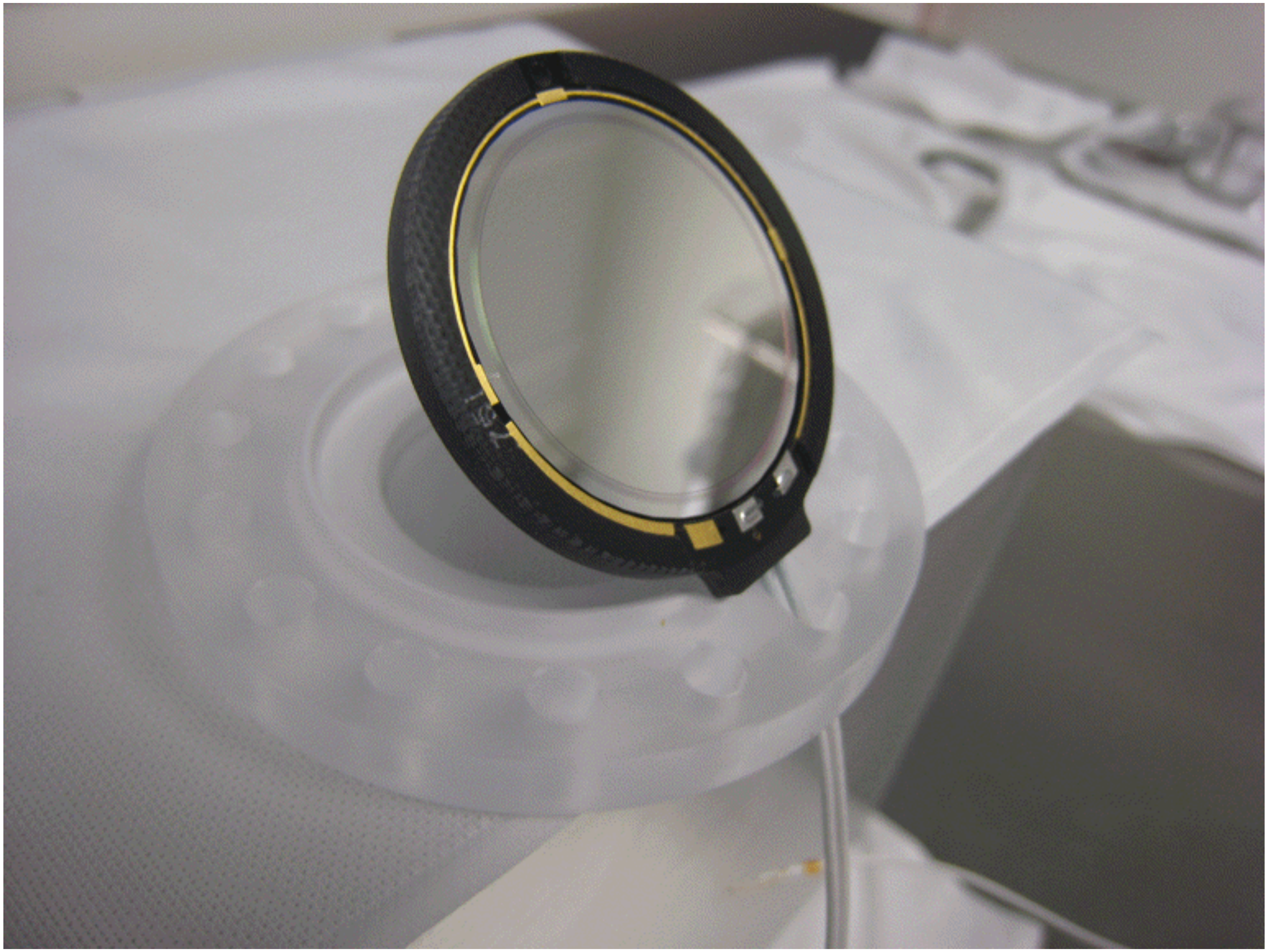

Proton Energy deposition in 1500 μm Si

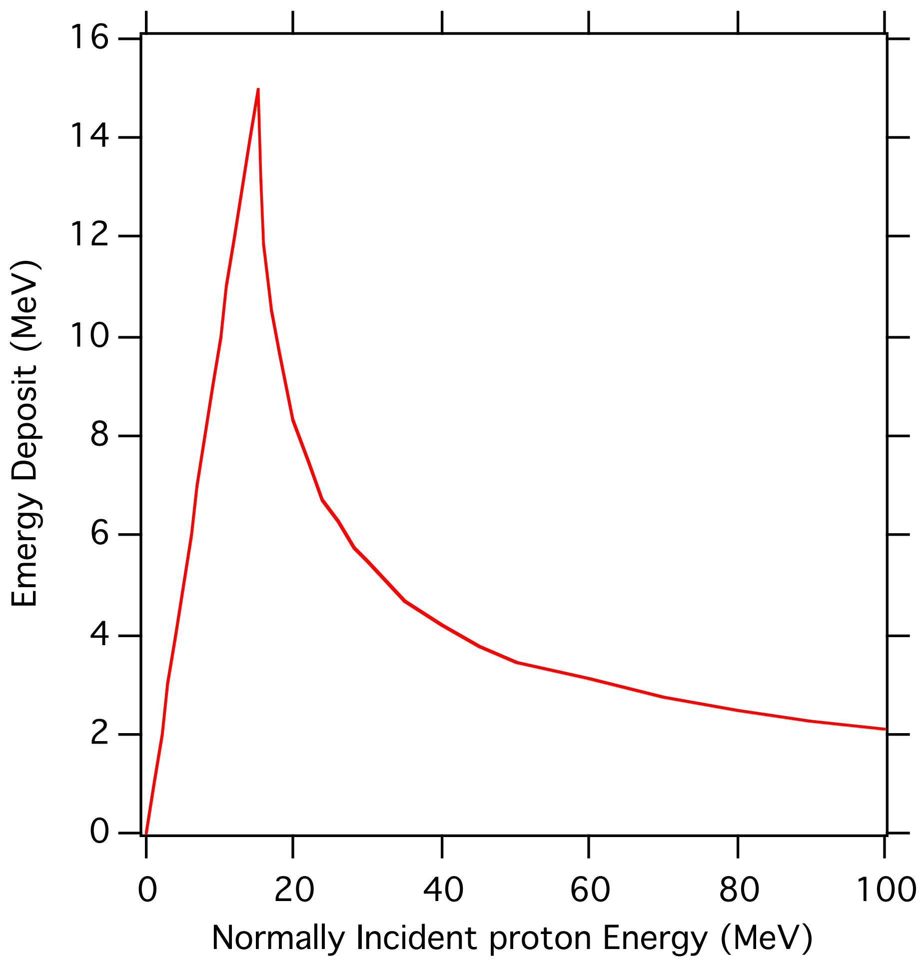

Measuring Energetic Charged Particles in Space

$\Delta E/\Delta x$

but

$\Delta x \sim \sec(\theta)$

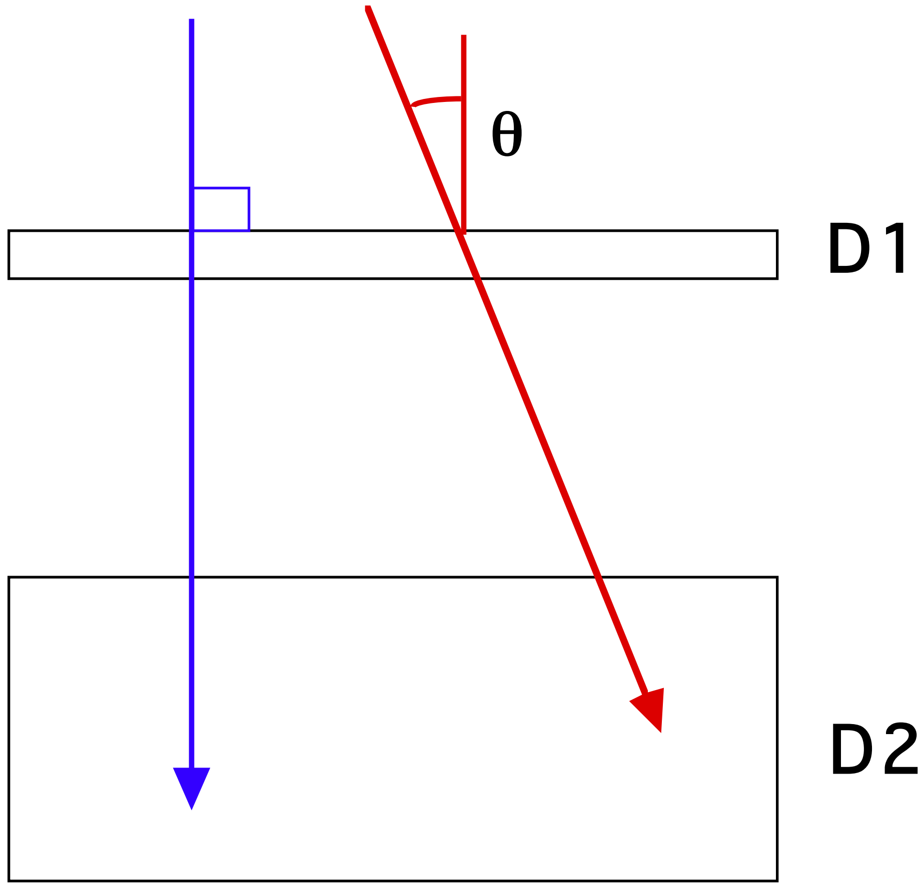

$E' = E'$

$\Delta E/\Delta x$ versus residual energy (E')

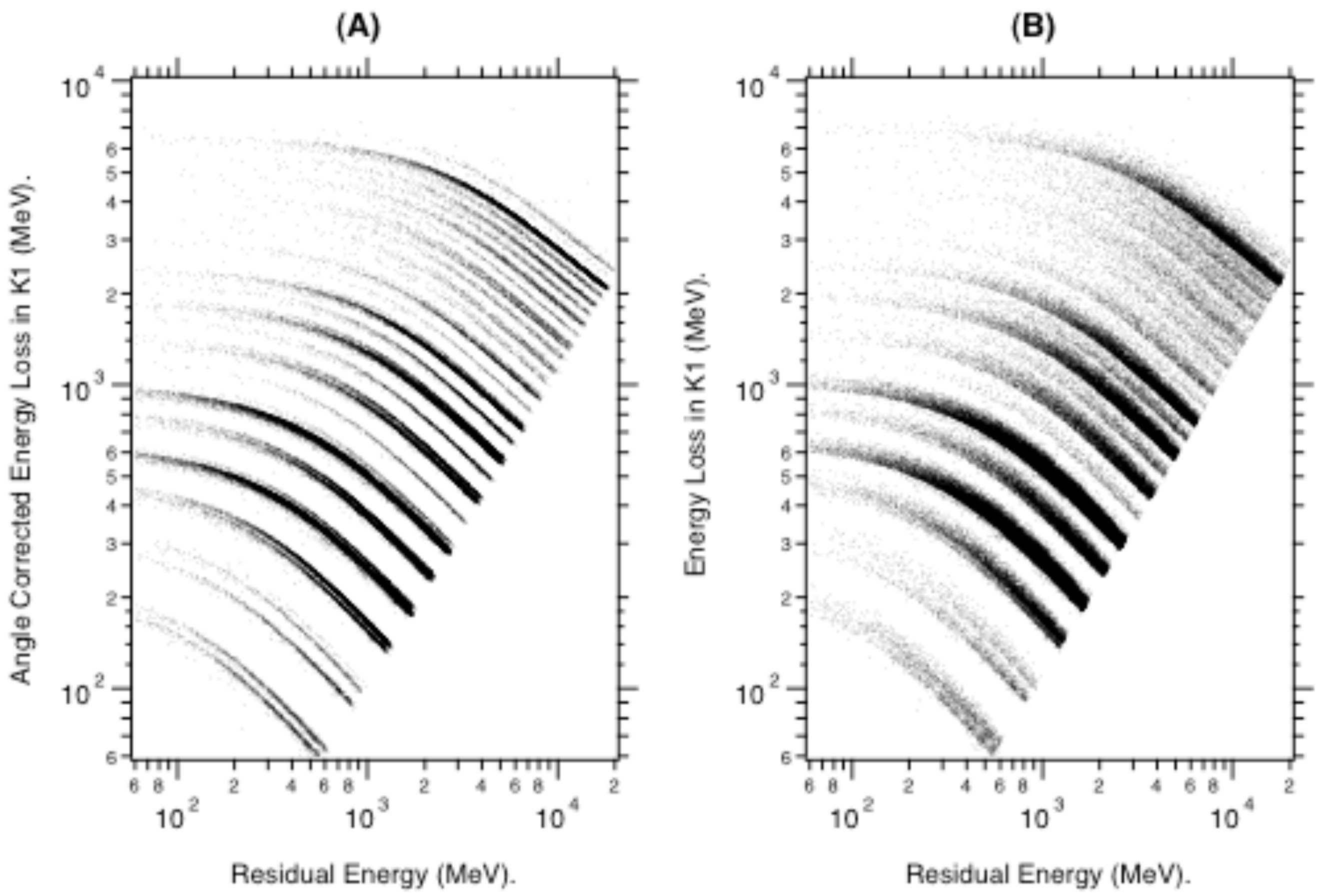

Ulysses HET flight data with (A) and without (B) correcting for particle angle of incidence—corrections need to identify elements.

Ulysses High Energy Telescope (HET)

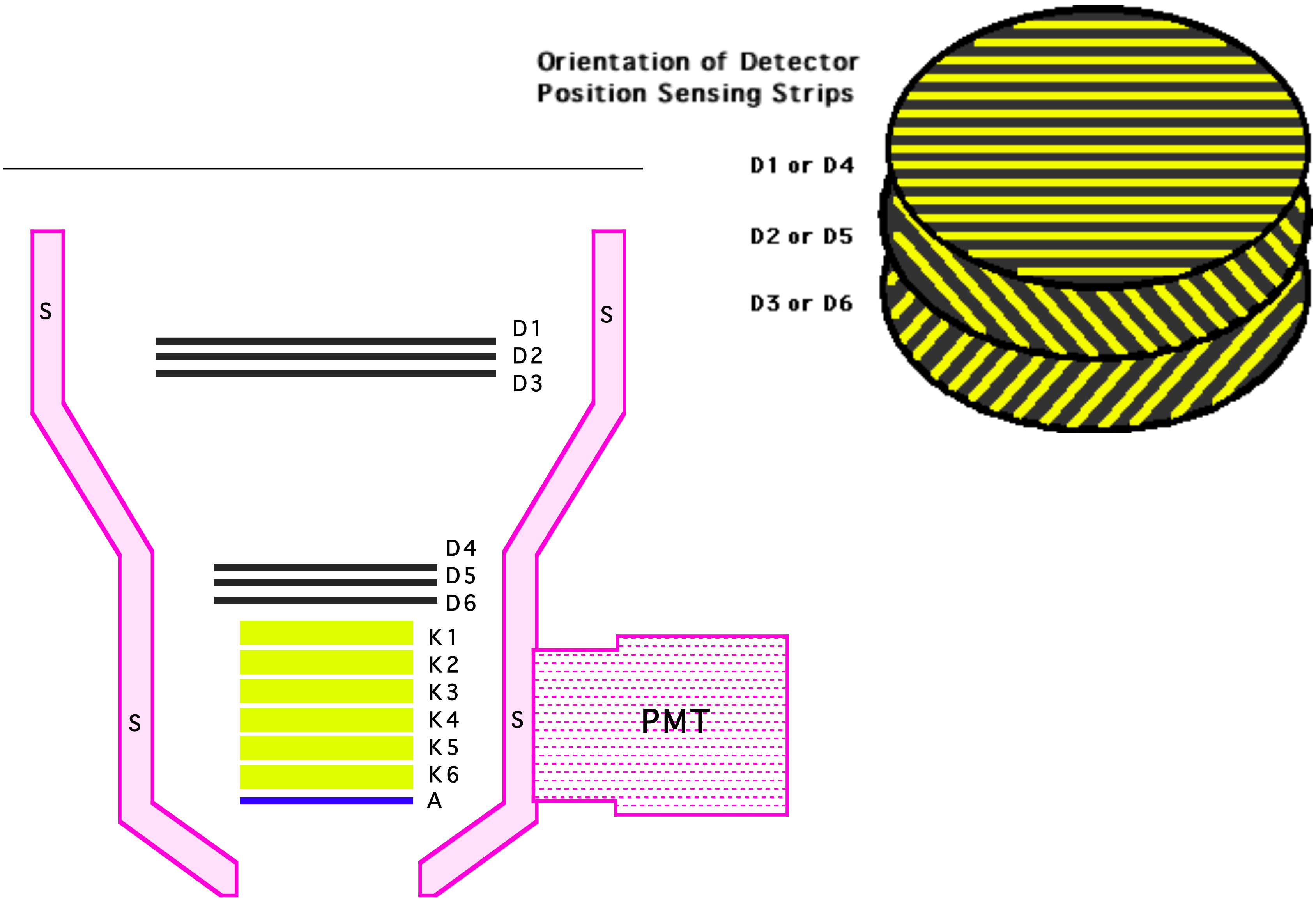

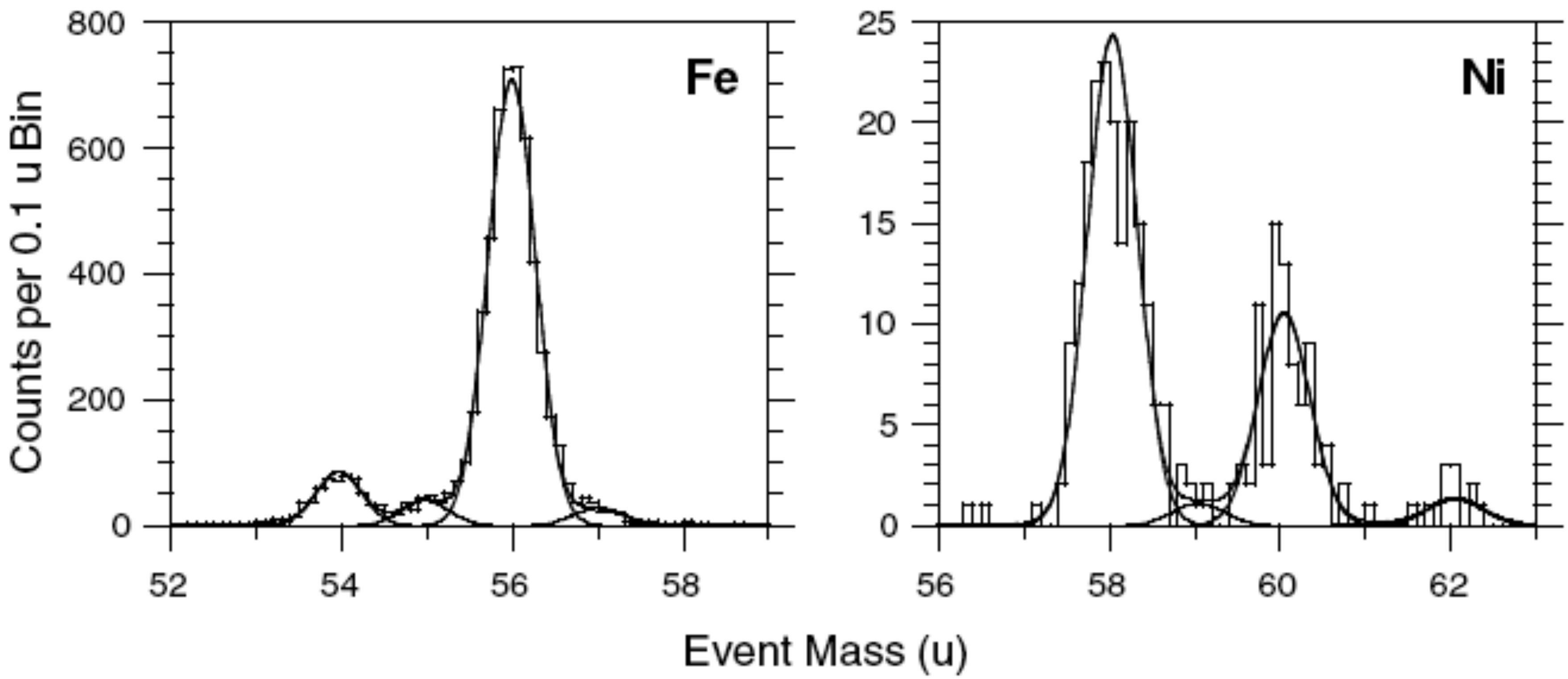

Fe
Ni
Counts per 0.1 u Bin
Event Mass (u)
800
600
400
200
0
25
20
15
10
5
0
52
54
56
58
56
58
60
62

Note ^{55}Fe

^{55}Fe is created by spallation with the ISM

At these energies (~1 GeV/u), ions are stripped

If not, it is after $^{56}Fe+p \rightarrow {}^{55}Fe+p+n$

^{55}Fe decays only by electron capture

(half-life 2.7 years)

It is stable in the cosmic rays

Exception when it picks up an electron

Then it decays (stripping time >> 2.7 ys)

SN 1987A

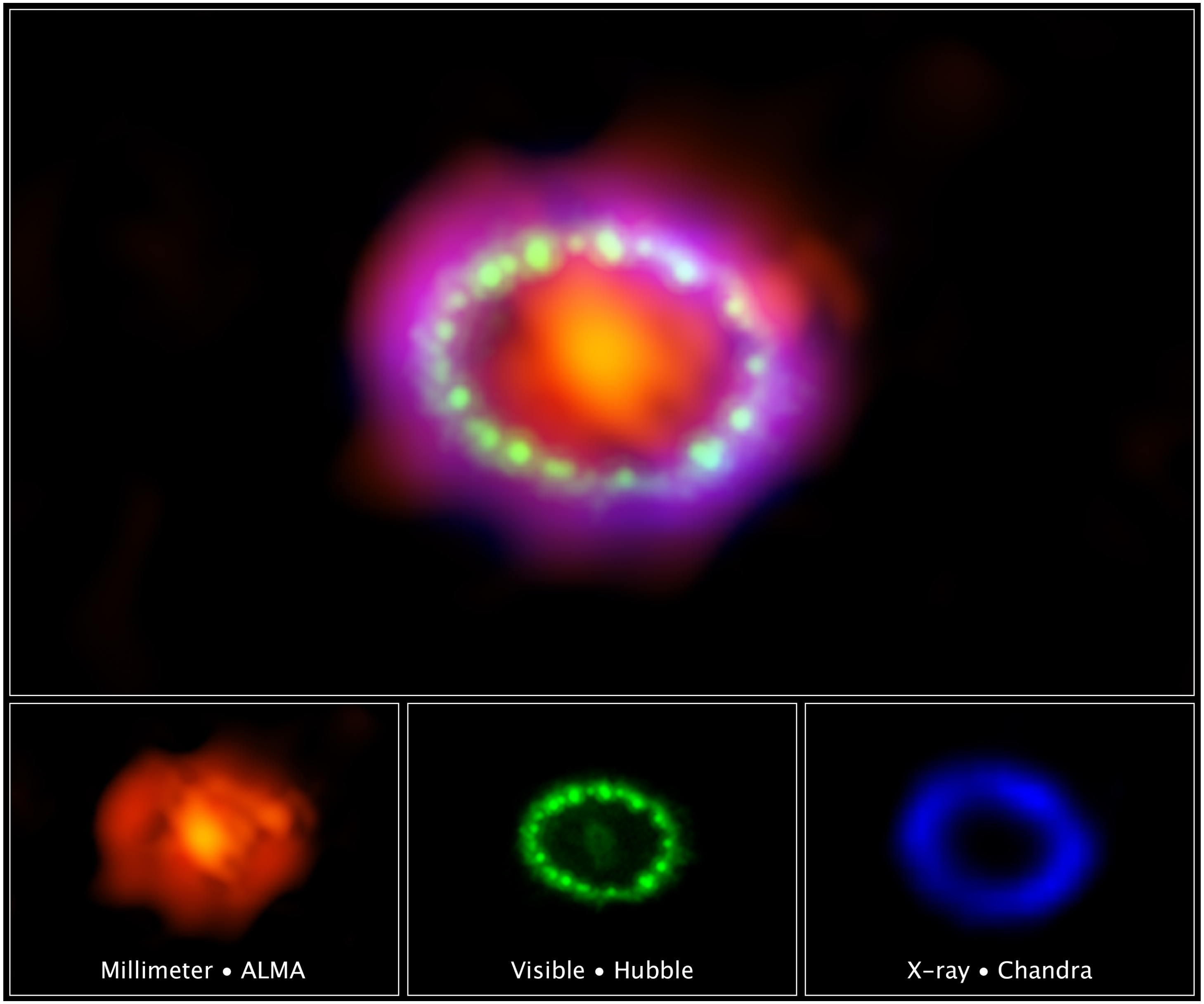

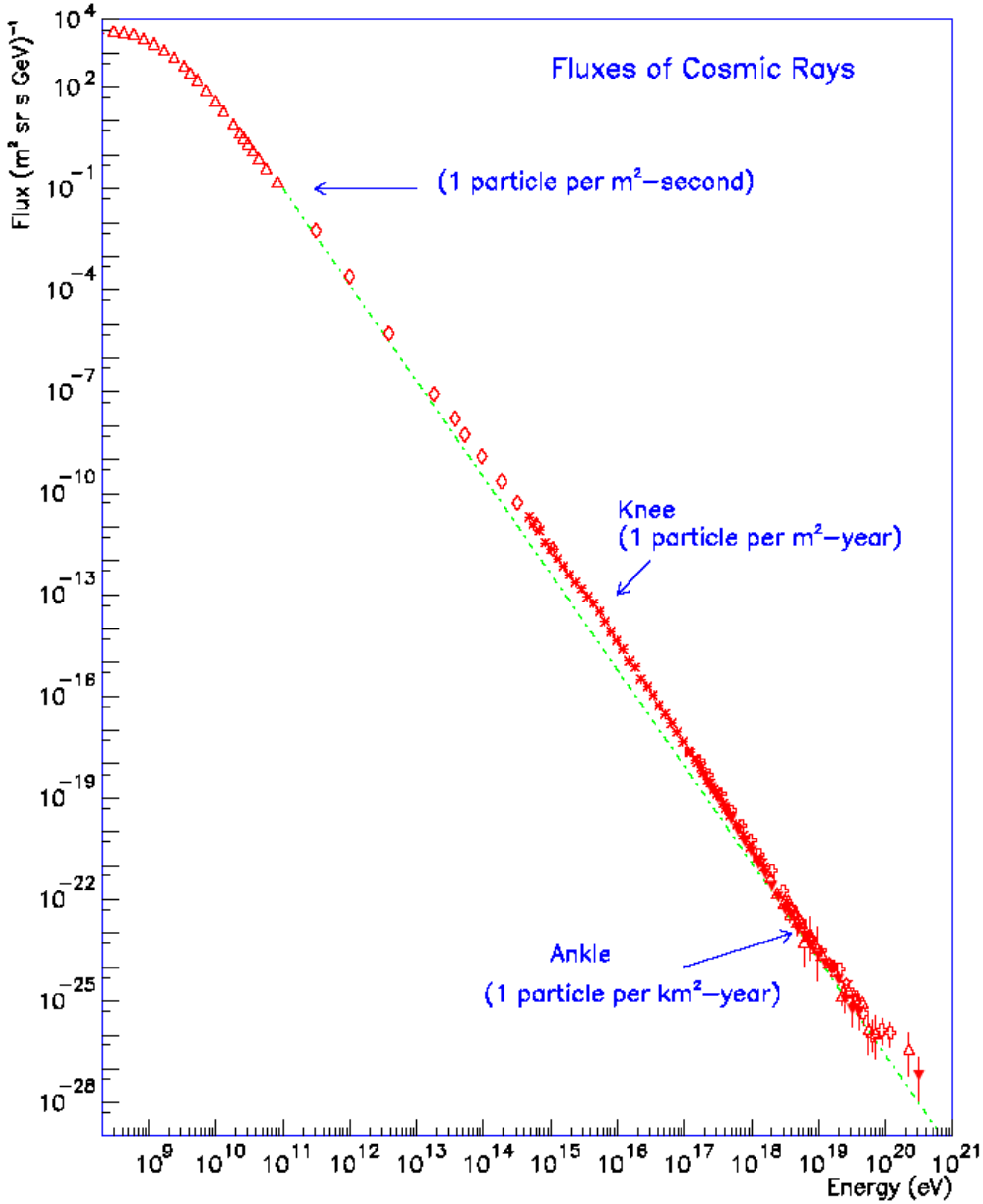

Figure 1. The all particle spectrum of cosmic rays - Cronin, Gaisser, Swordy 1997

The GCR spectrum continues as a power, in energy (index of about -2.7)

Highest energy cosmic rays have the kinetic energy of a major league baseball.

Cosmic Rays

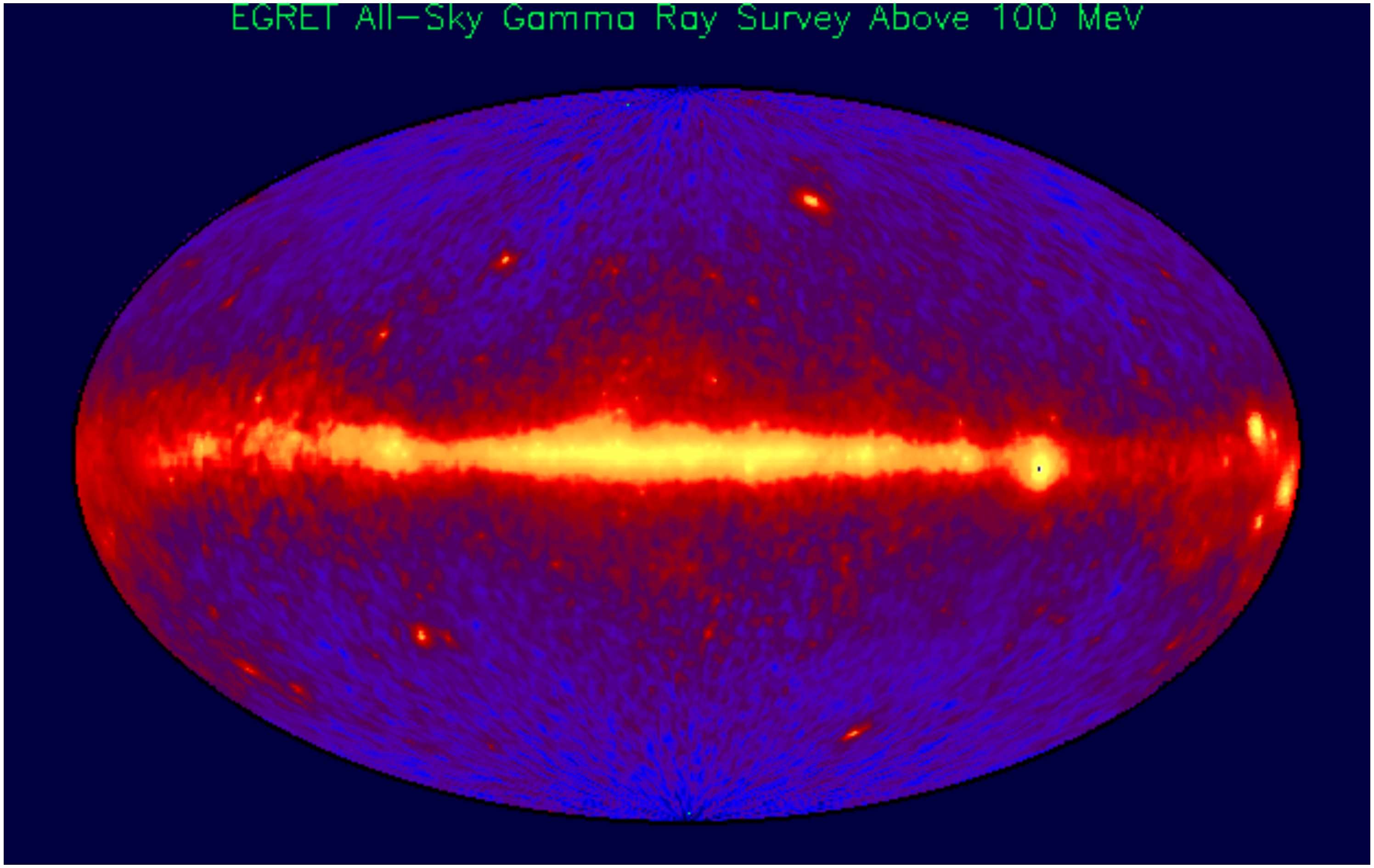

Galactic Cosmic Ray Chemical Abundances Compared to Solar System Abundances

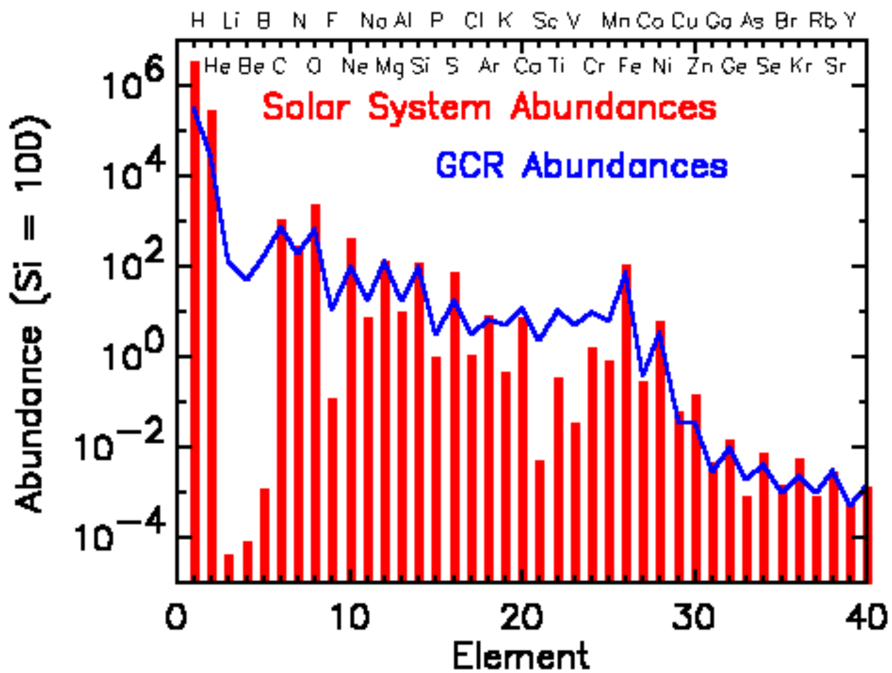

GCR abundance of rare elements enhance by spallation of heavier nuclides. These secondary elements (Li, Be, B, sub-Fe) are a measure of the amount of ISM the cosmic rays traverse

$n + N\text{-}14 \rightarrow C\text{-}14 + p$

Carbon-14 dating

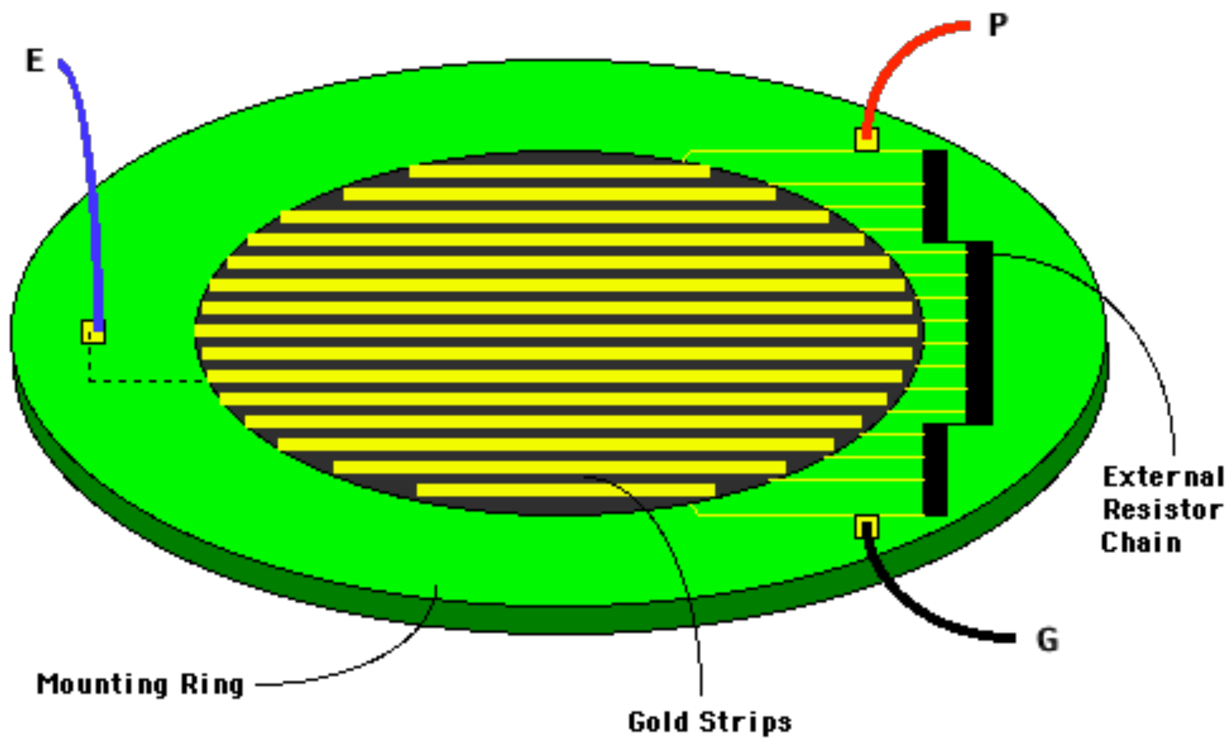
E
P
External
Resistor
Chain
G
Mounting Ring
Gold Strips

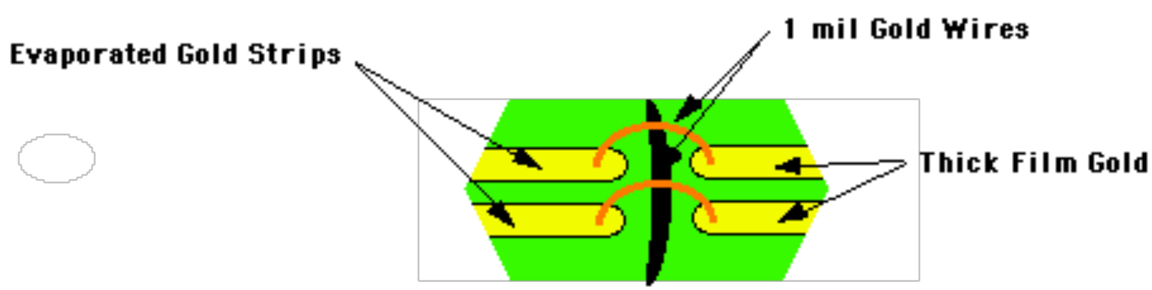
1 mil Gold Wires
Evaporated Gold Strips
Thick Film Gold

Inset

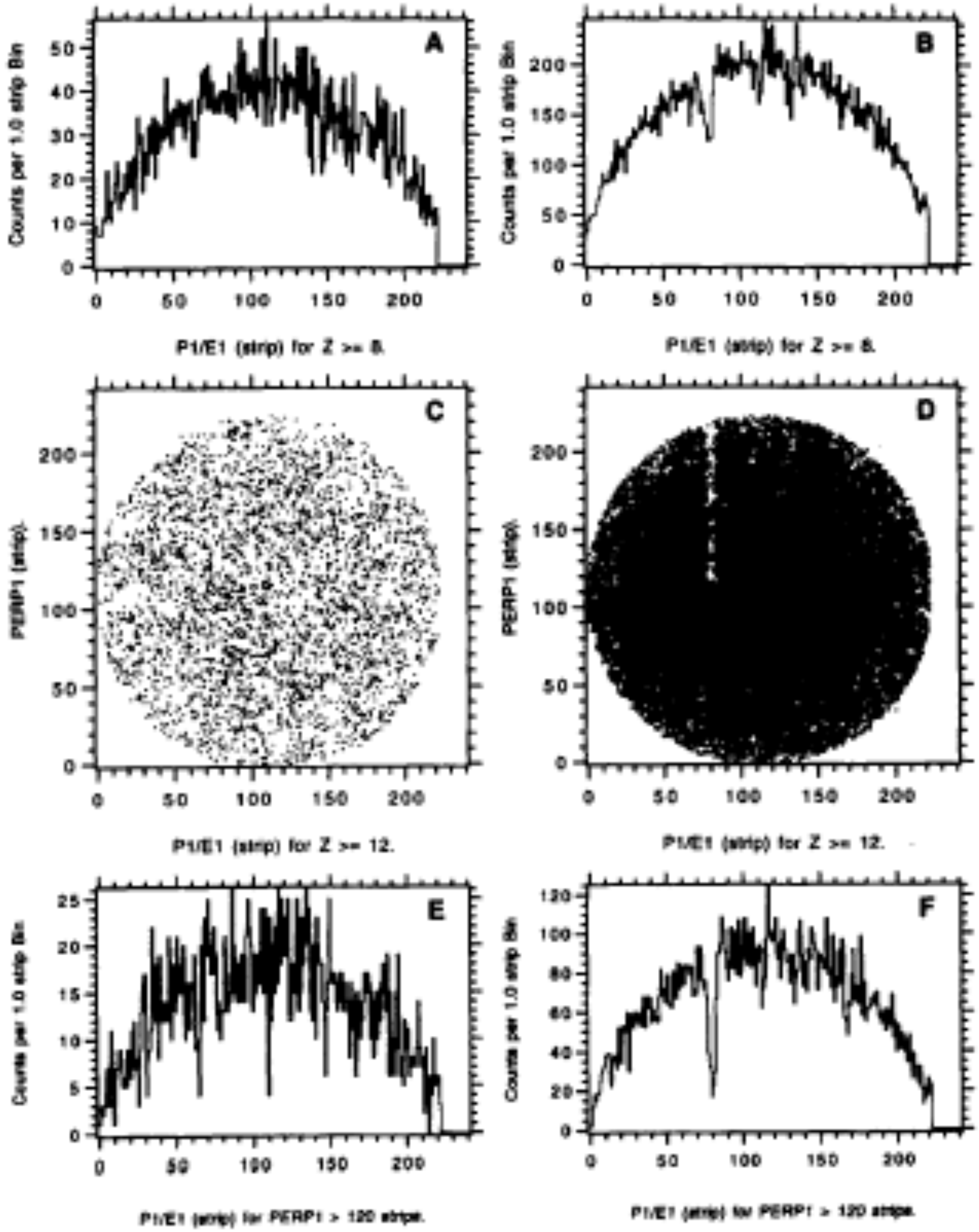
A
B
C
D
E
F
Counts per 1.0 strip Bin
PERP1 (strip)
P1/E1 (strip) for Z >= 8.
P1/E1 (strip) for Z >= 12.
P1/E1 (strip) for PERP1 > 120 strips.

Nuclear Instruments and Methods in Physics Research A 378 (1996) 526–528

NUCLEAR INSTRUMENTS & METHODS IN PHYSICS RESEARCH Section A

ELSEVIER

Effects of an apparent space dust impact on a position sensing solid state detector aboard the Ulysses spacecraft

J.J. Connell*

The Laboratory for Astrophysics and Space Research, The Enrico Fermi Institute, The University of Chicago, Chicago IL 60637, USA

Received 6 February 1996

Abstract

The High Energy Telescope (HET) is part of the COsmic and Solar Particle INvestigation (COSPIN) aboard the Ulysses spacecraft. The Ulysses mission is to explore the Heliosphere in three dimensions by passing over the polar regions of the sun. Ulysses achieved it present high inclination (> 80°) solar orbit via a gravitational sling-shot around Jupiter. During or proximate to Jovian encounter, the HET suffered an apparent dust impact. The dust particle entered through the telescope aperture windows and damaged the top position sensing solid state detector. This paper discusses the evidence of the impact in the data, and the effect of the impact on the detector.

1. Introduction

The High Energy Telescope (HET) aboard Ulysses is a high resolution cosmic ray isotope spectrometer described in detail elsewhere [1]. Six position sensing detectors (PSDs) are crucial to the HET's ability to resolve different isotopes up to Fe [2–4]. Each PSD consists of a Li drifted Silicon detector of ~1100 μm thickness with a series of gold strip electrodes deposited on the top and a solid electrode on the bottom (Fig. 1). The nominal pitch of the strips is 317.5 μm, with 222 strips on D1–D3 and 143 strips on D4–D6. A 1 mil. gold wire connects each strip to an external resister network which provides charge division. One end of the network is grounded, while the other is pulse height analyzed ("P" measurement), as is the bottom electrode ("E" measurement), when an event coincidence is triggered. To first order, the ratio of P/E is proportional the position in one dimension of the cosmic ray event. Thus each PSD measures event position in one dimension.

The PSDs are arranged in two sets of three at the top (front) of the HET detector stack. The PSDs in each set of three are oriented at 60° so that a failure in flight of any detector would have a minimal effect on the trajectory

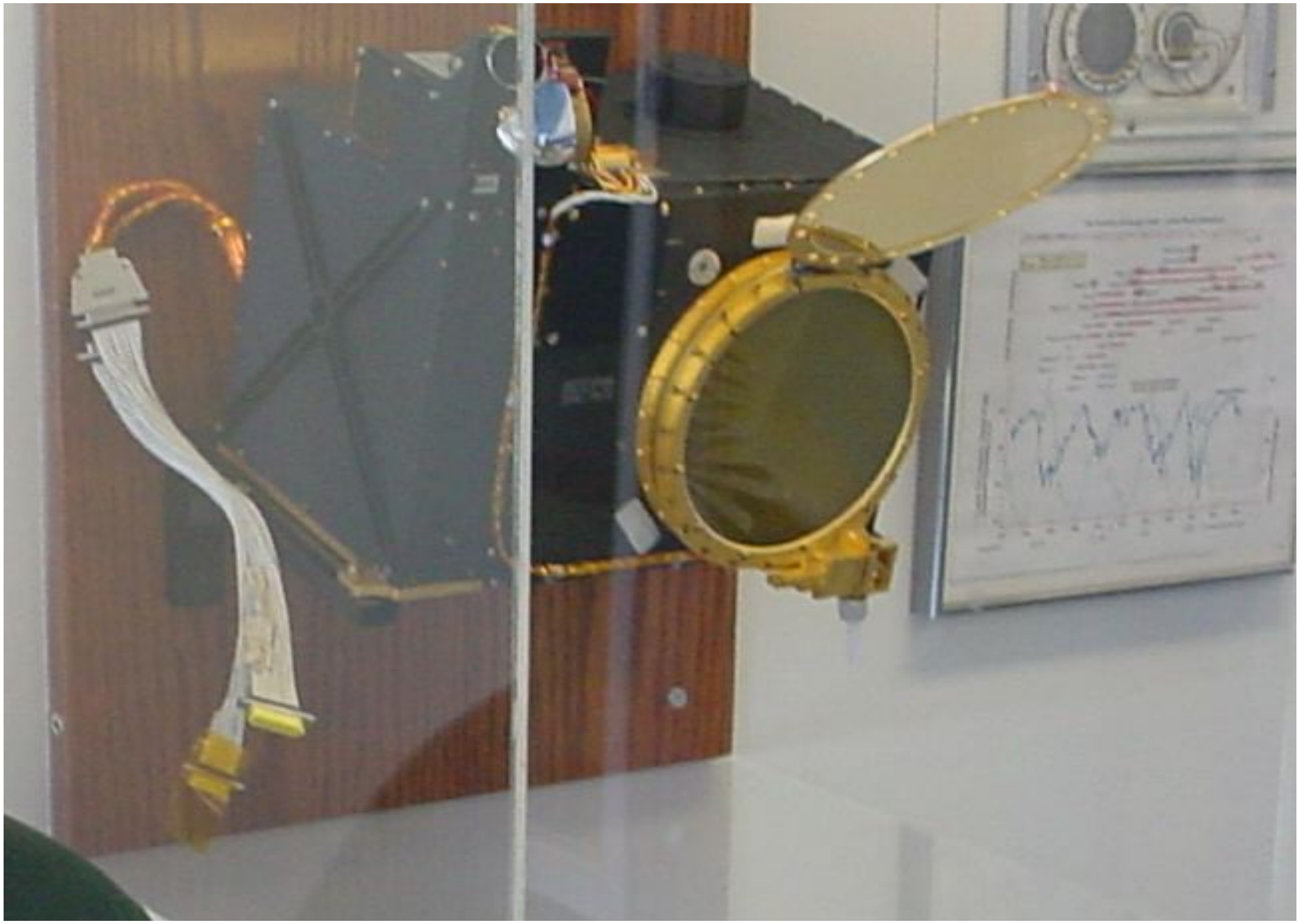

Ulysses HET Flight Spare, UNH Morse Hall 4th Floor

KING GEORGE V

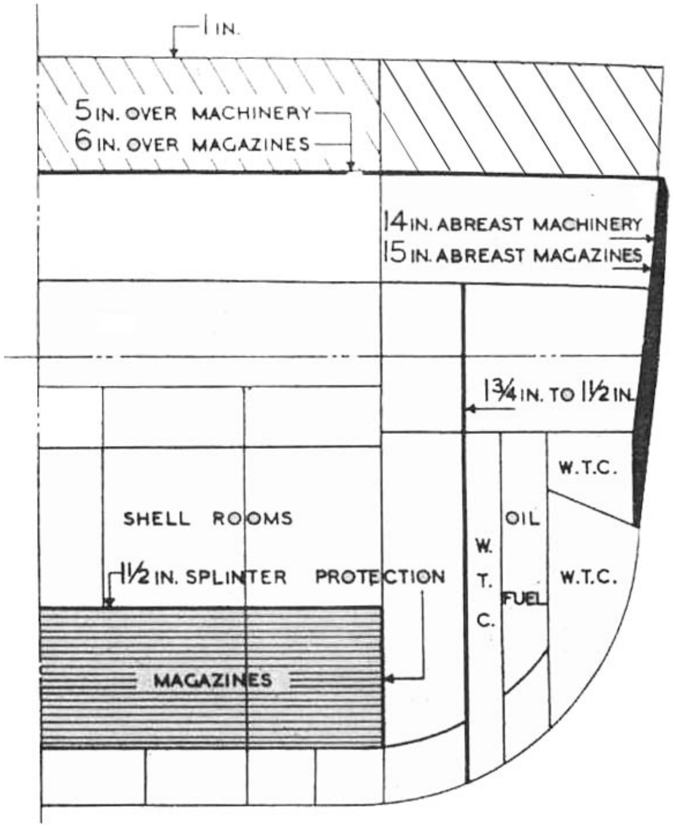

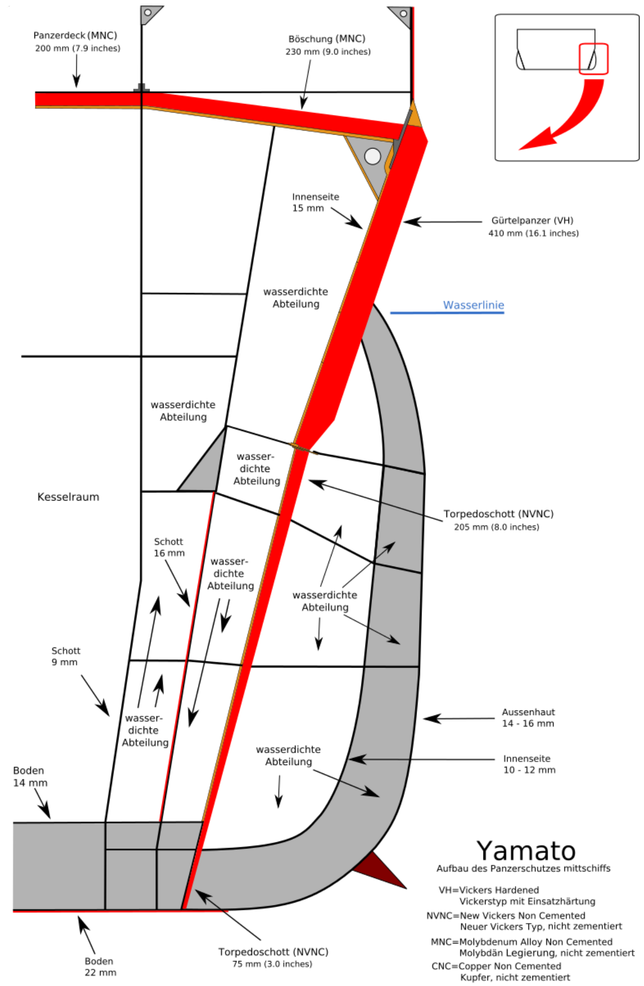

KING GEORGE V

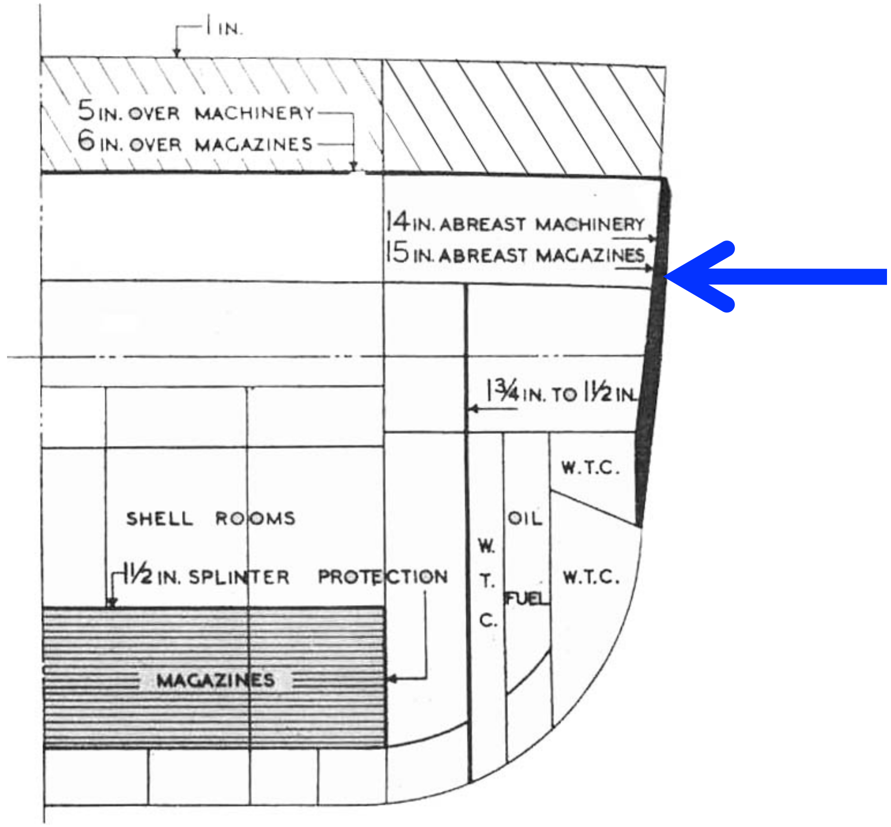

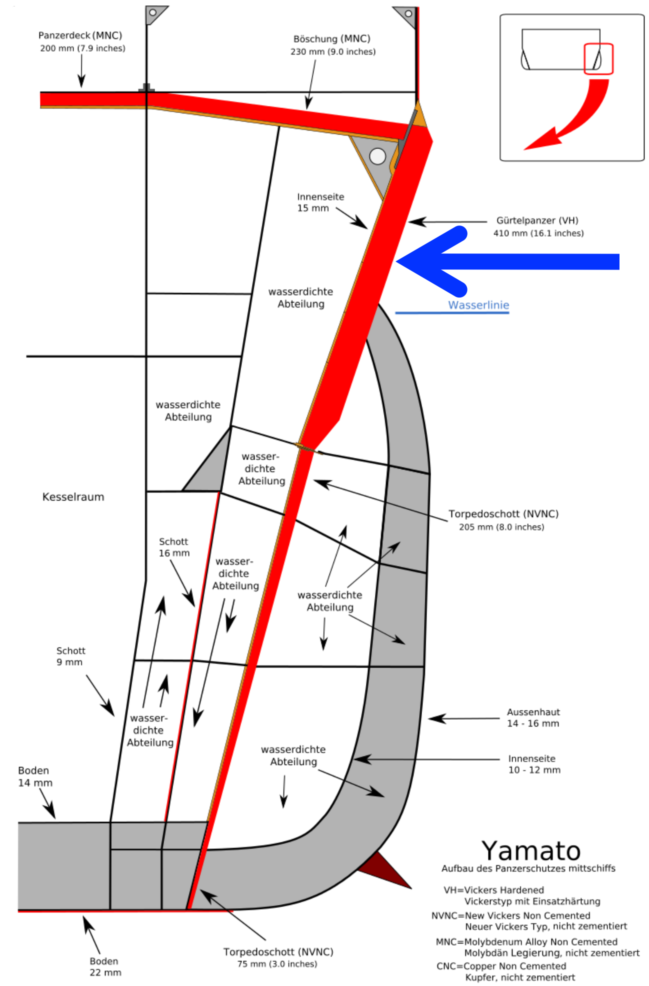

$\sim\sec(\phi)$

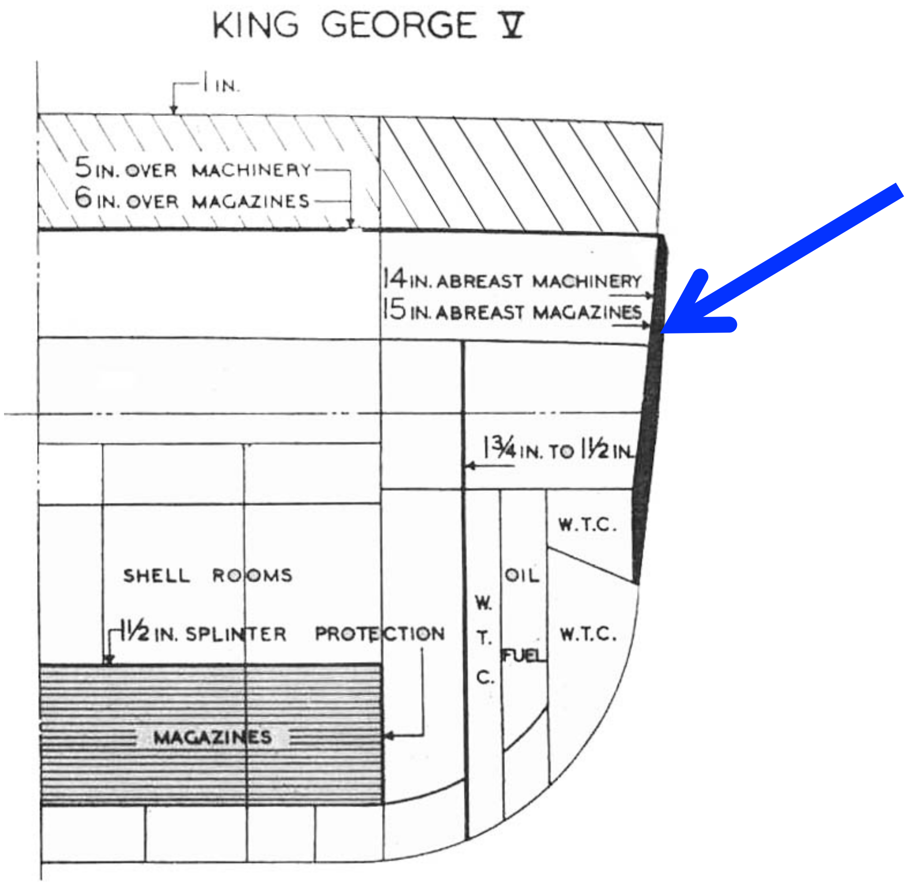

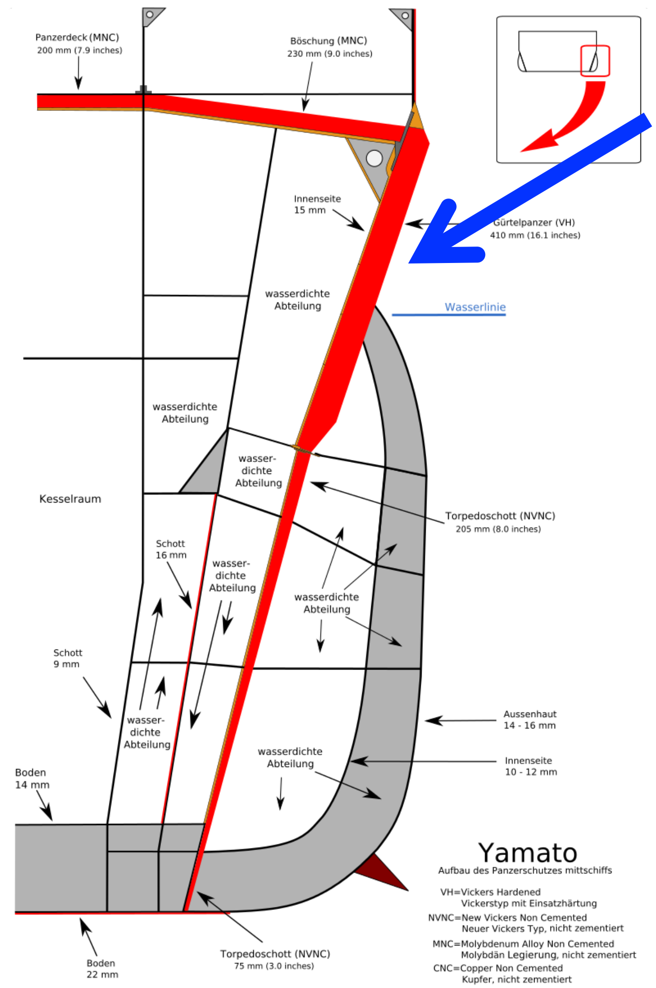

$\sim\sec(\theta)$

$\sim\sec(\theta+\phi)$

Angle Detecting Inclined Sensor (ADIS)

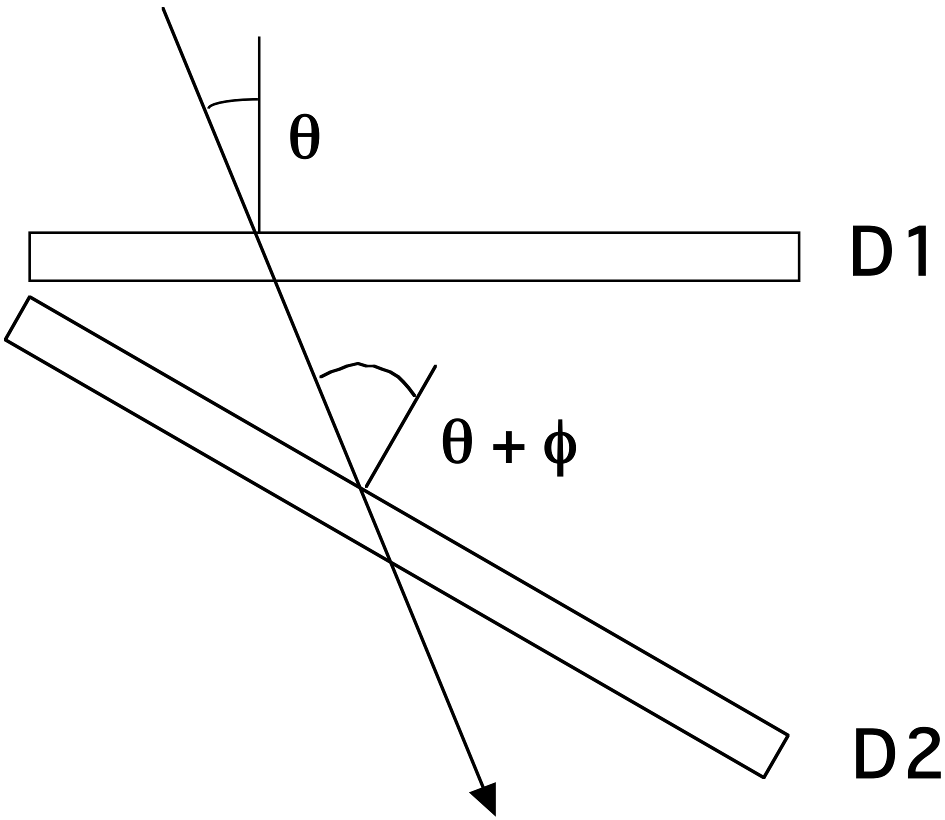

$$\frac{E_1}{E_2} = \frac{\sec(\theta)}{\sec(\theta + \phi)}$$

ADIS Test Model

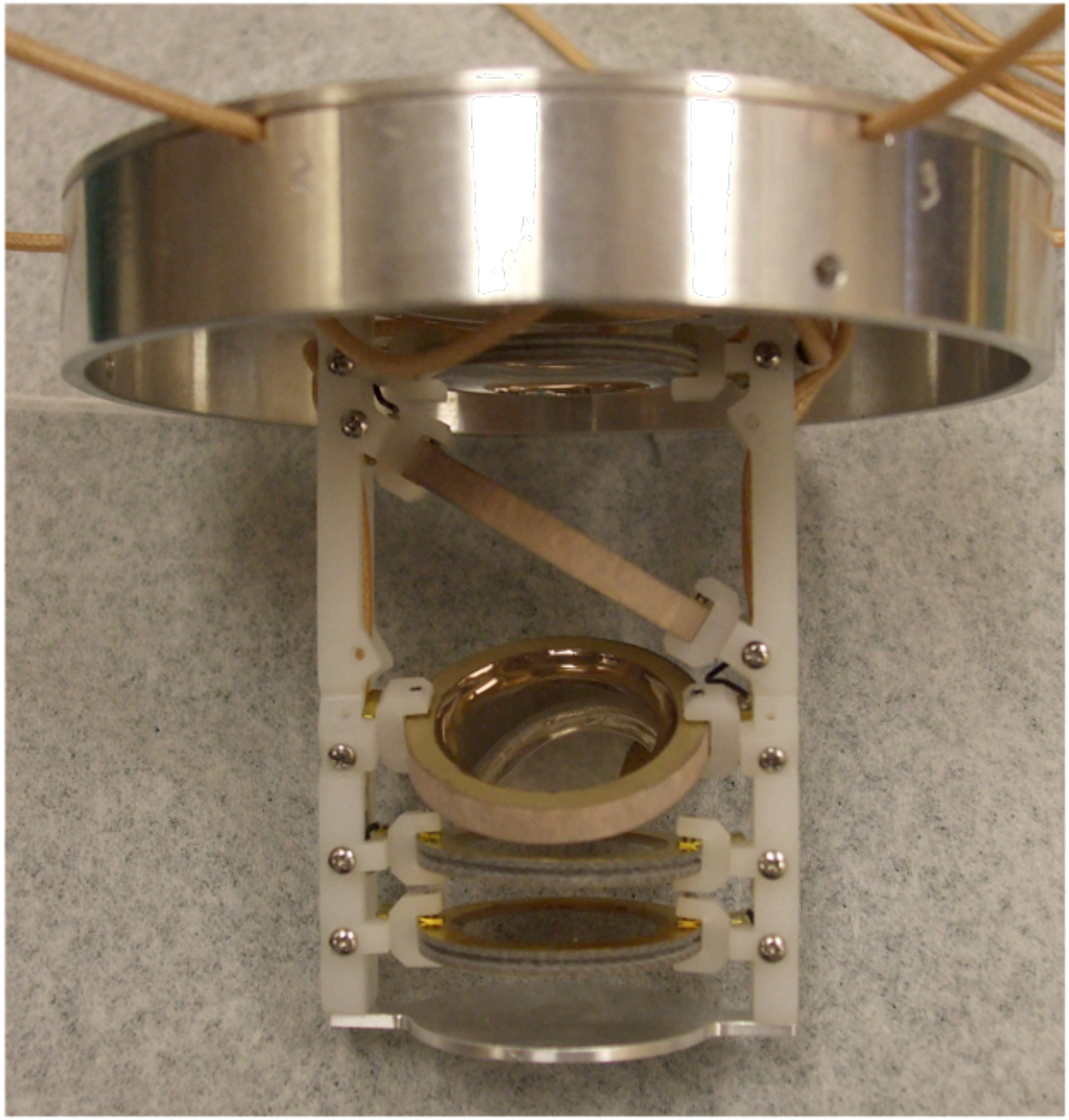

This is, of course, all
“From a Different Angle”!

This is, of course, all
“From a Different Angle”!

“He who would pun would pick a pocket.”
Alexander Pope, 1729

Angle Detecting Inclined Sensor (ADIS)

- Different geometry in telescope stack
- Uses standard Si detector technology
- Low risk
- Low mass
- Low power
- On-board event processing possible

An ADIS based Instrument was selected for the High Energy Particle Sensor (HEPS) for National Polar-orbiting Operational Environmental Satellite System (NPOESS)

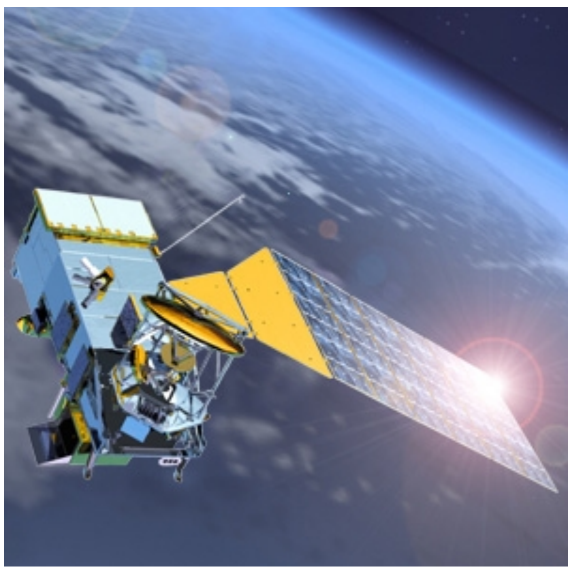

J. J. Connell, PI on HEPS


R.I.P.

Energetic High Ion Sensor (EHIS) for GOES-R

First Space Weather Instrument to measure heavy ions

C. Lopate, PI on EHIS

EHIS

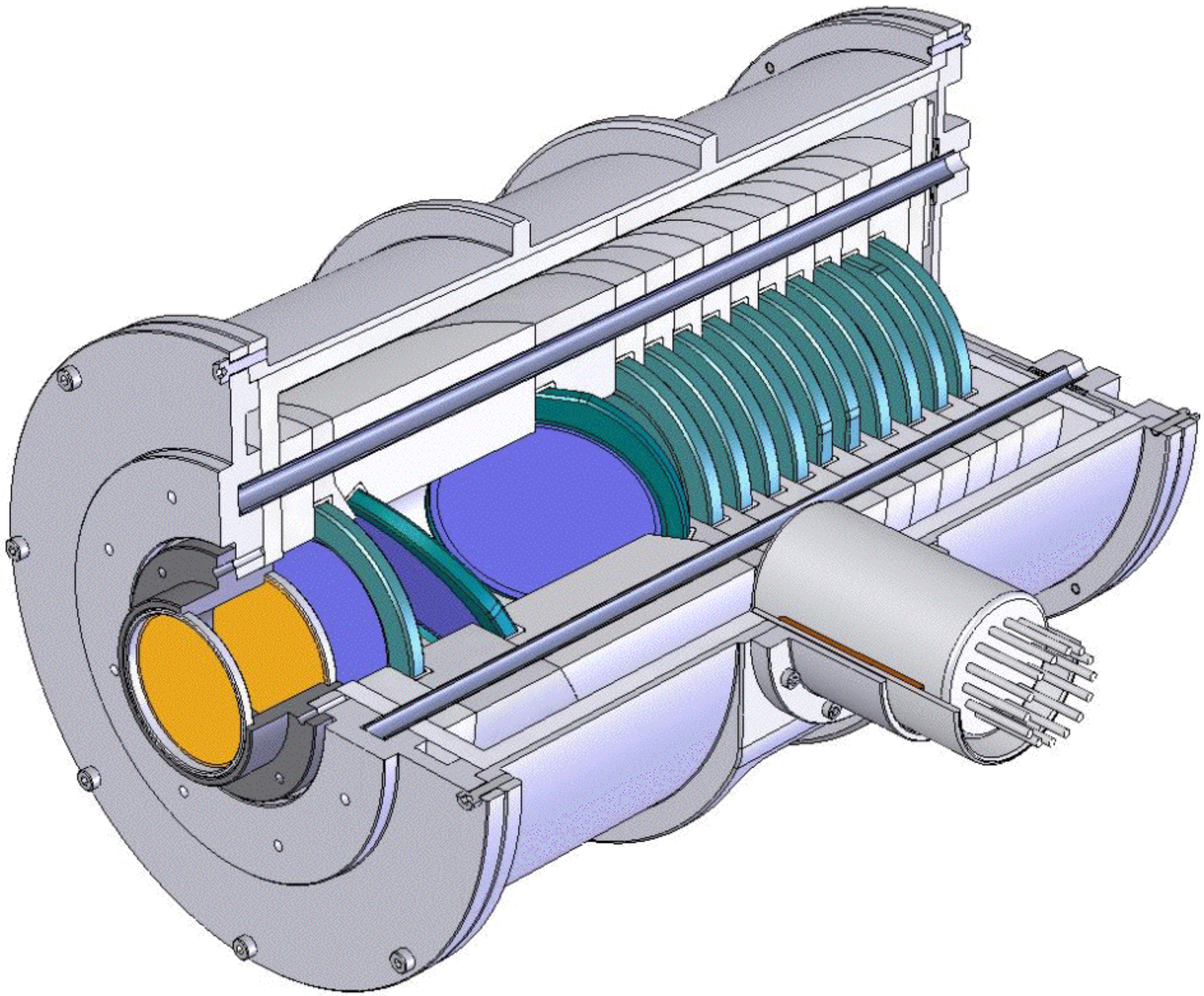

EHIS FM1

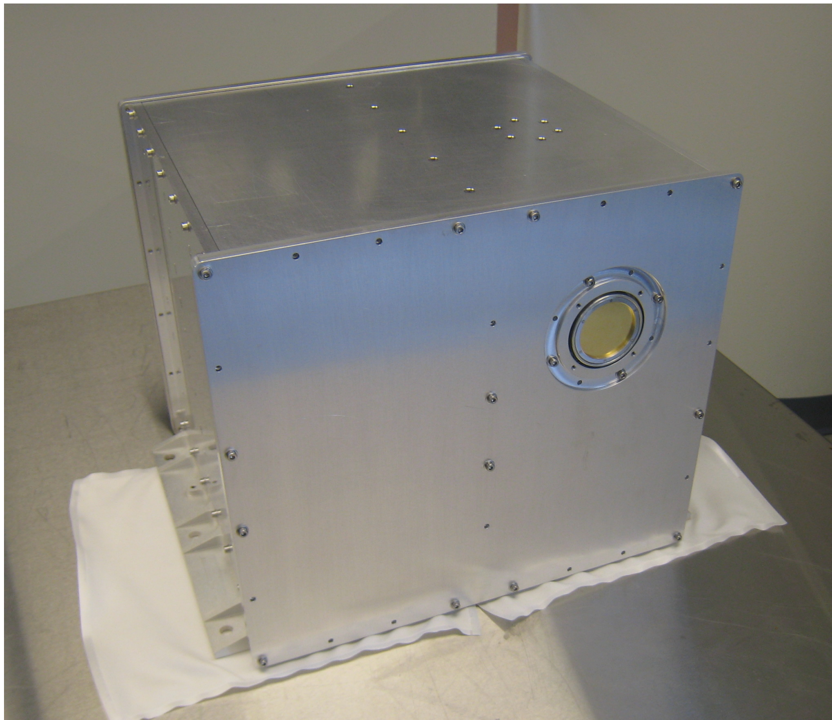

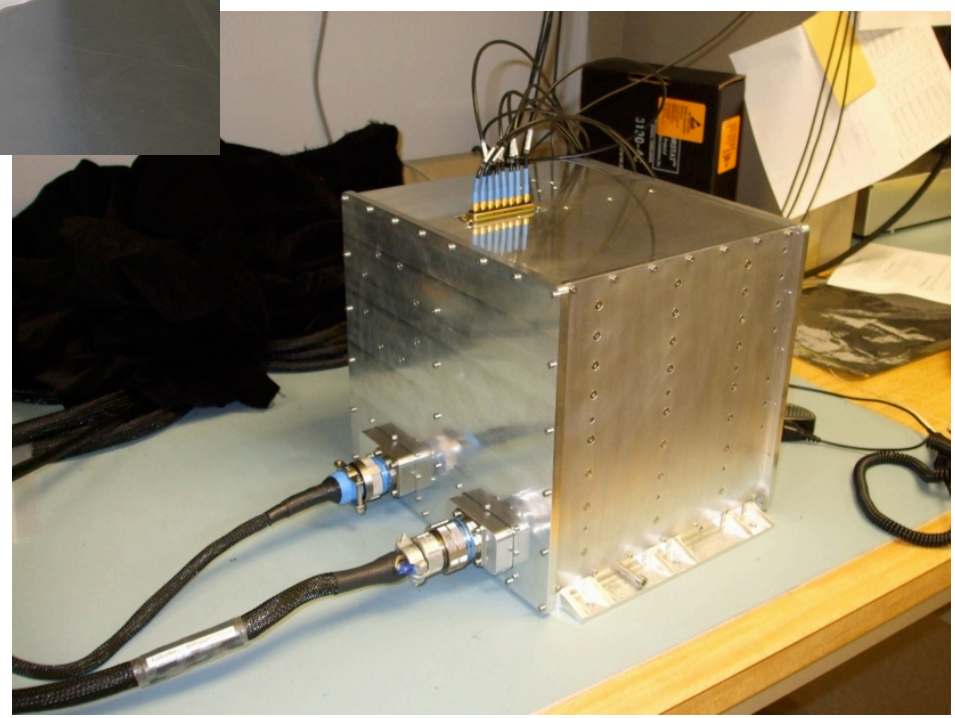

EHIS FM1 MSU NSCL Heavy Ion Calibration

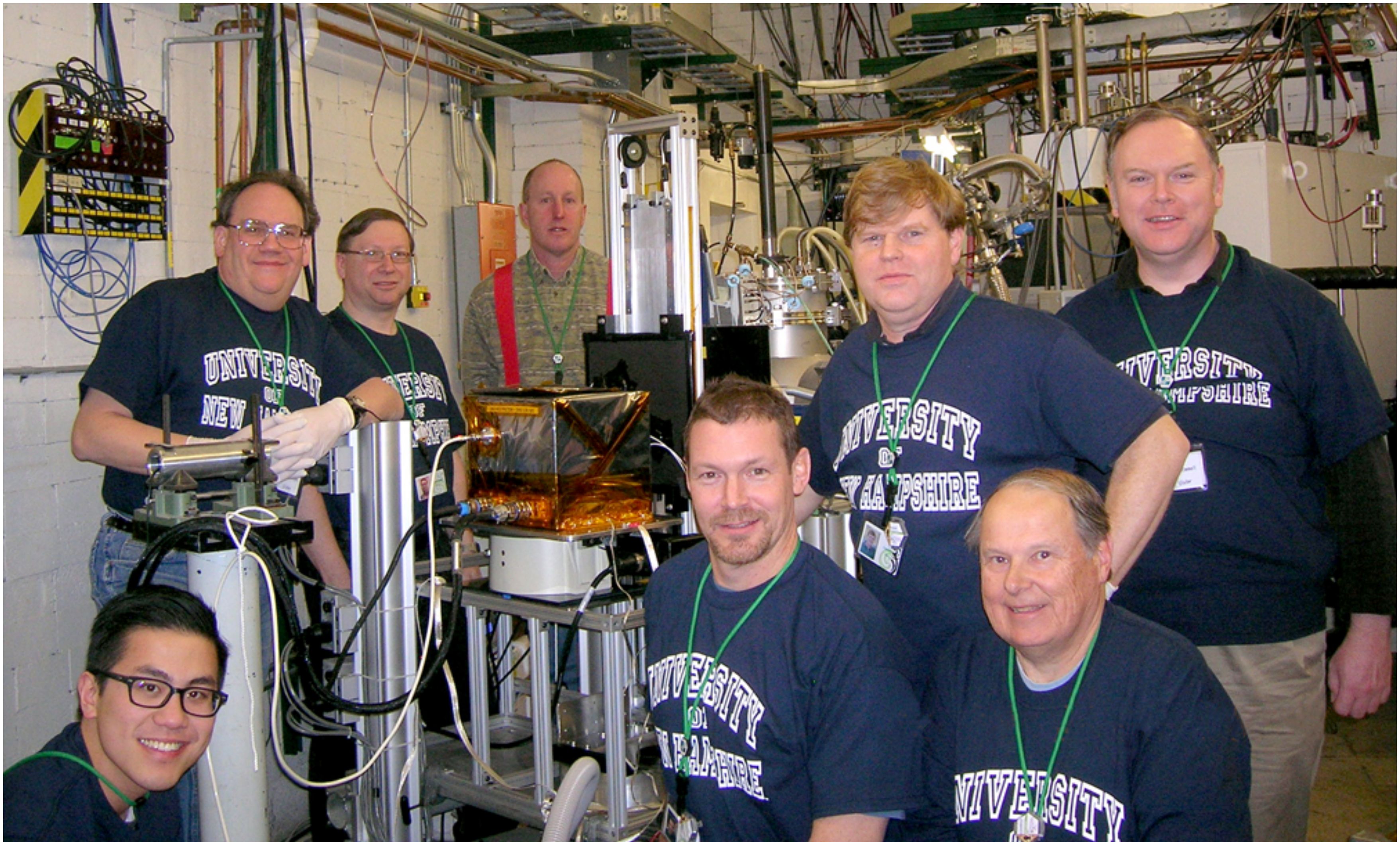

GOES-R (-16)
19 Nov. 2016

GOES-S (-17)
1 March 2018

Charged Particle Spectrum

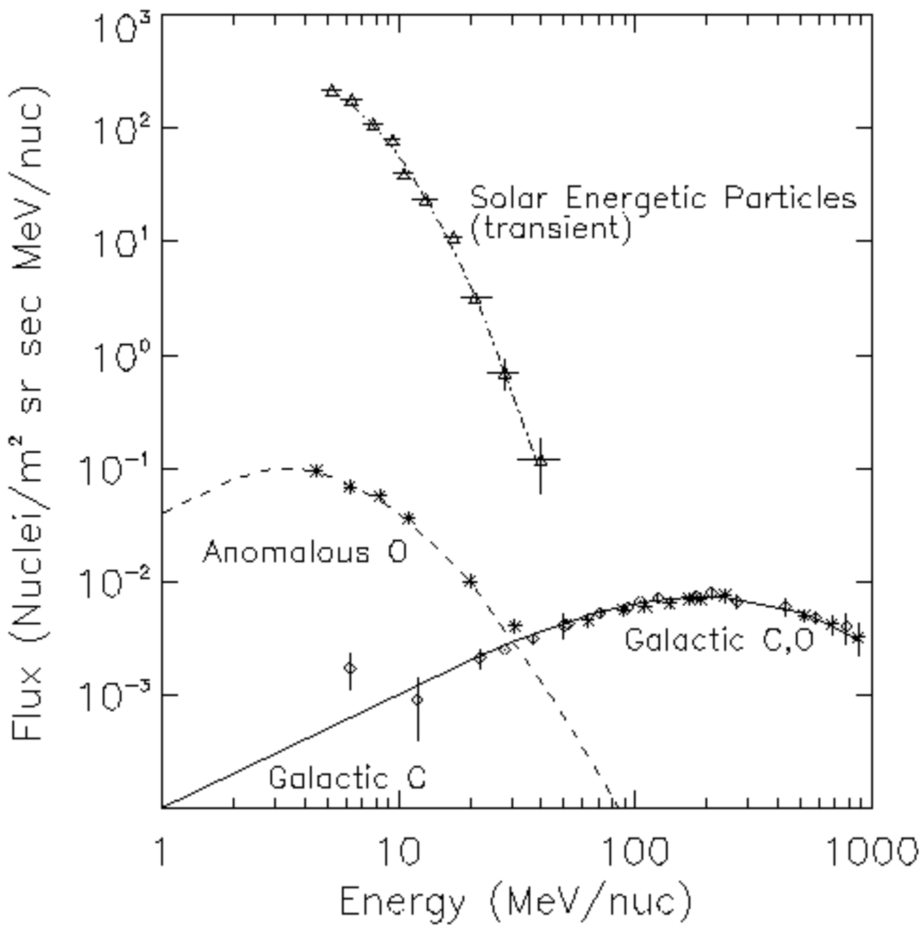

Ions not marked by source

Energy and timing help separate sources

Charge state also:

- AC singly charged
- GCR full stripped
- SEP partially stripped

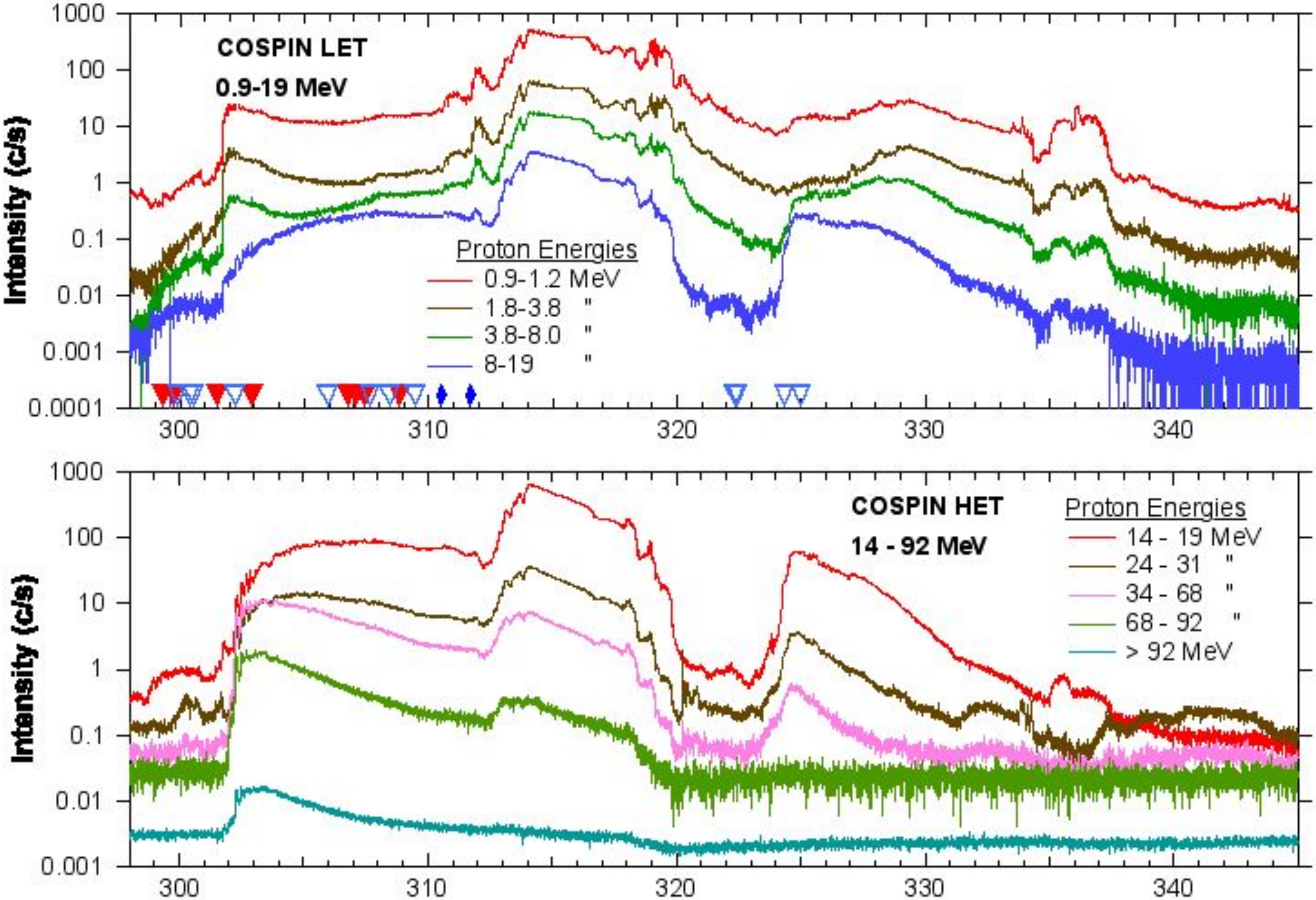

COSPIN LET
0.9-19 MeV
Intensity (c/s)
Proton Energies
0.9-1.2 MeV
1.8-3.8 "
3.8-8.0 "
8-19 "
1000
100
10
1
0.1
0.01
0.001
0.0001
300
310
320
330
340
COSPIN HET
14 - 92 MeV
Proton Energies
14 - 19 MeV
24 - 31 "
34 - 68 "
68 - 92 "
> 92 MeV

Uncooperative Local Star

Six month post-launch data GOES-16/EHIS

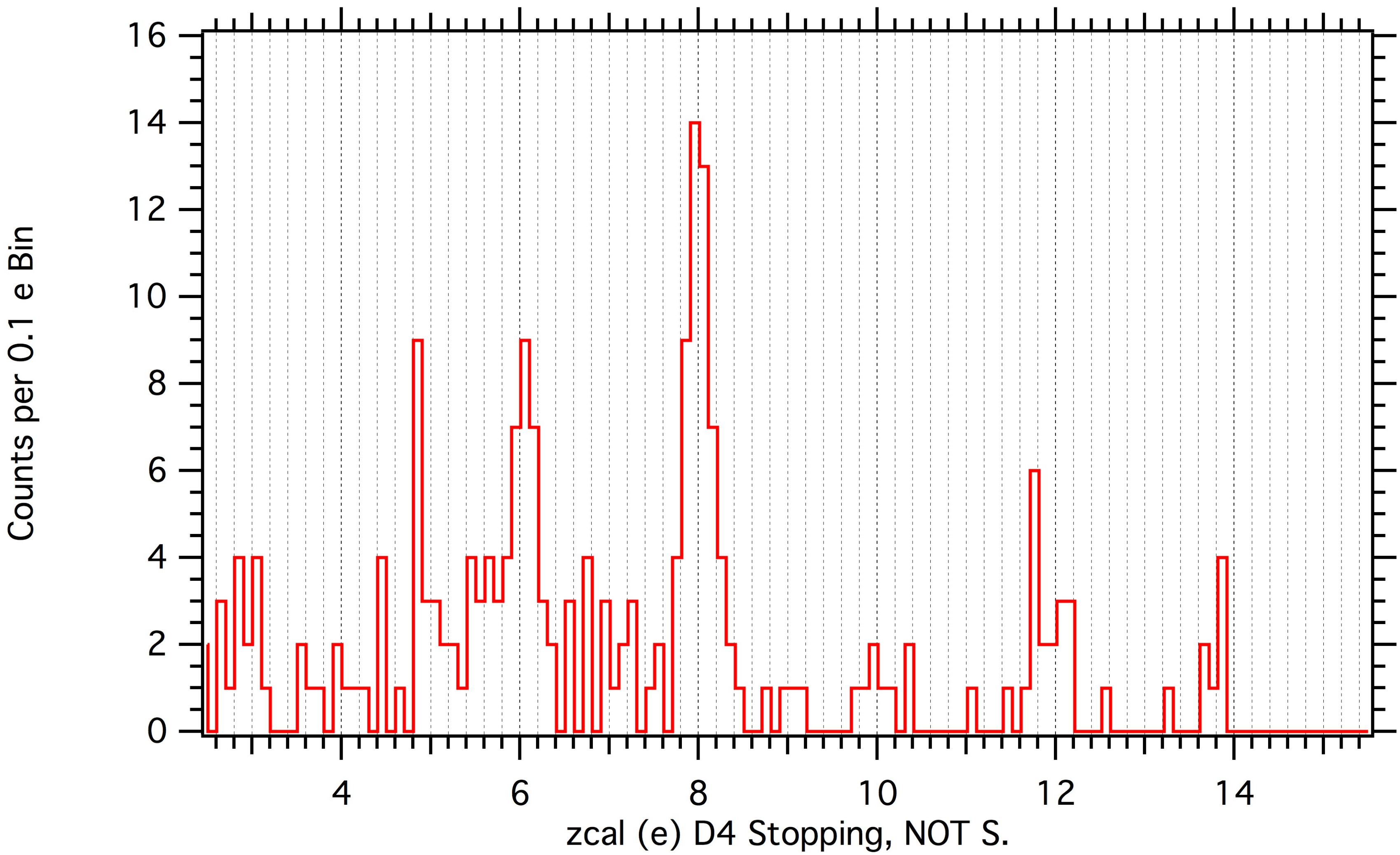

EHIS on GOES-16

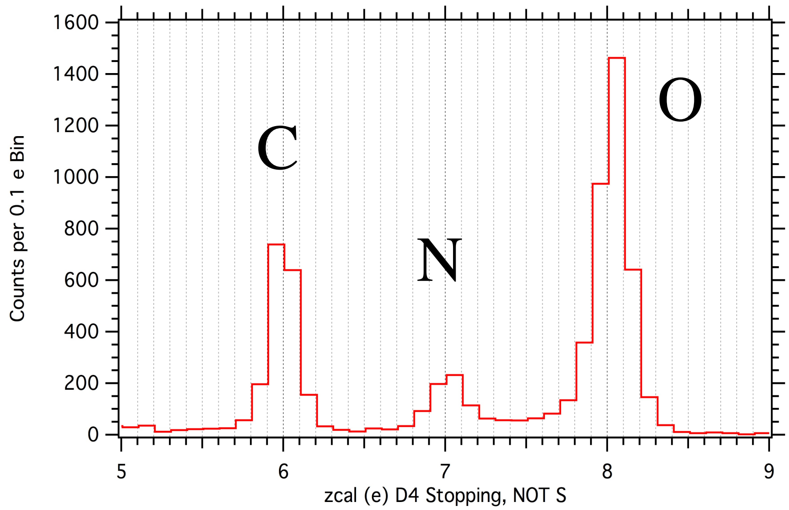

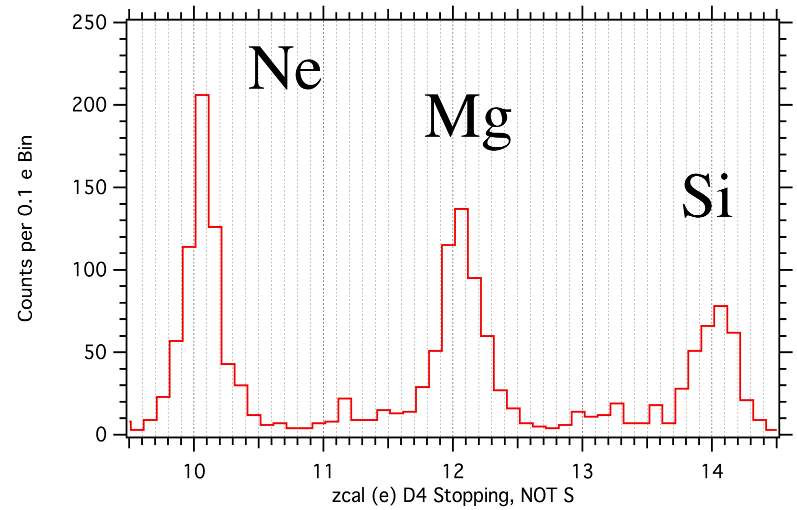

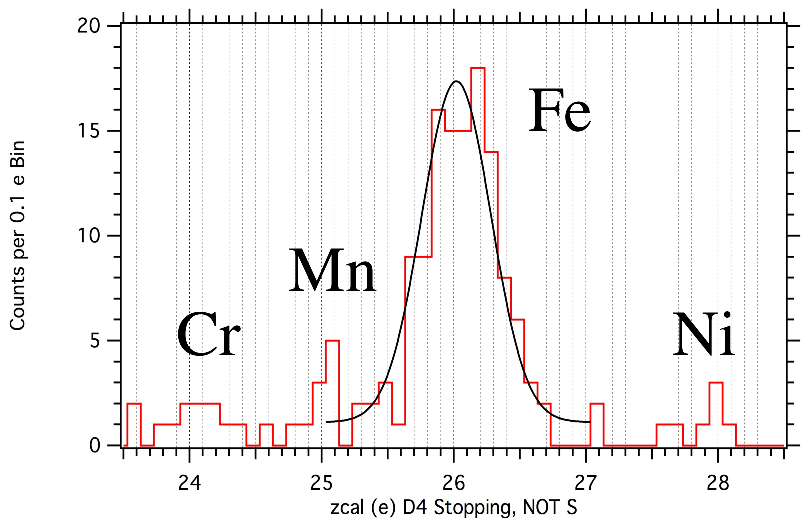

Finally, solar particle events
September 2017
Modest but hard spectrum
~85% of data shown

EHIS Results for the 10 September 2017 Solar Particle Event

- While there have been very few large energetic particle events during the past year, there have been three smaller events.
- The upper left figure show the raw counts for the Solar Particle Event of 10 September 2017.
  - Individual peaks are observed for C, N, O, Ne, Mg, Si, S and Fe.
- The upper right figure shows the calculated fluences for several ion species (Carbon, Nitrogen, Oxygen and Iron) from the ACE/SIS instrument at the L1 point, and the SEISS/EHIS instrument in geostationary orbit.
- Where counts are available, EHIS extends the energy range of measurements by about an order of magnitude above the SIS instrument.

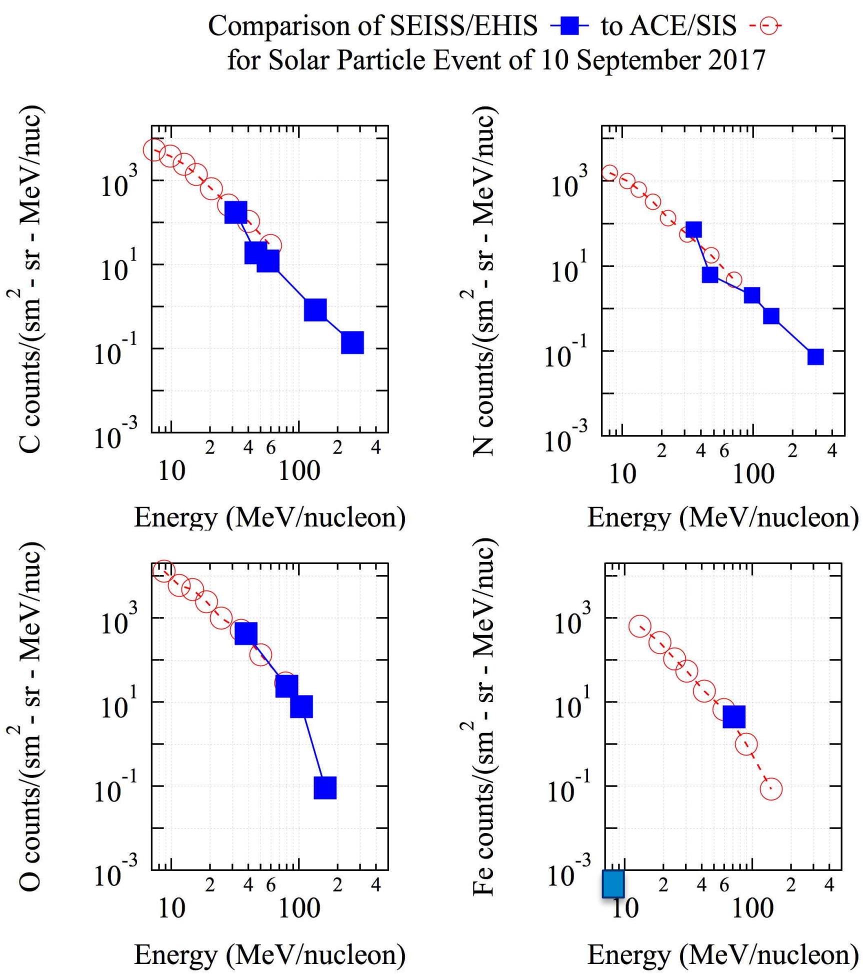

EHIS offers science quality data on an operational mission

Advantages:

- Two more EHIS in the queue
    - 2021 for GOES-T launch
- Fifth (spare) built and calibrated

Disadvantages:

- No funding for science
- Need to apply elsewhere
- Extreme risk-aversion

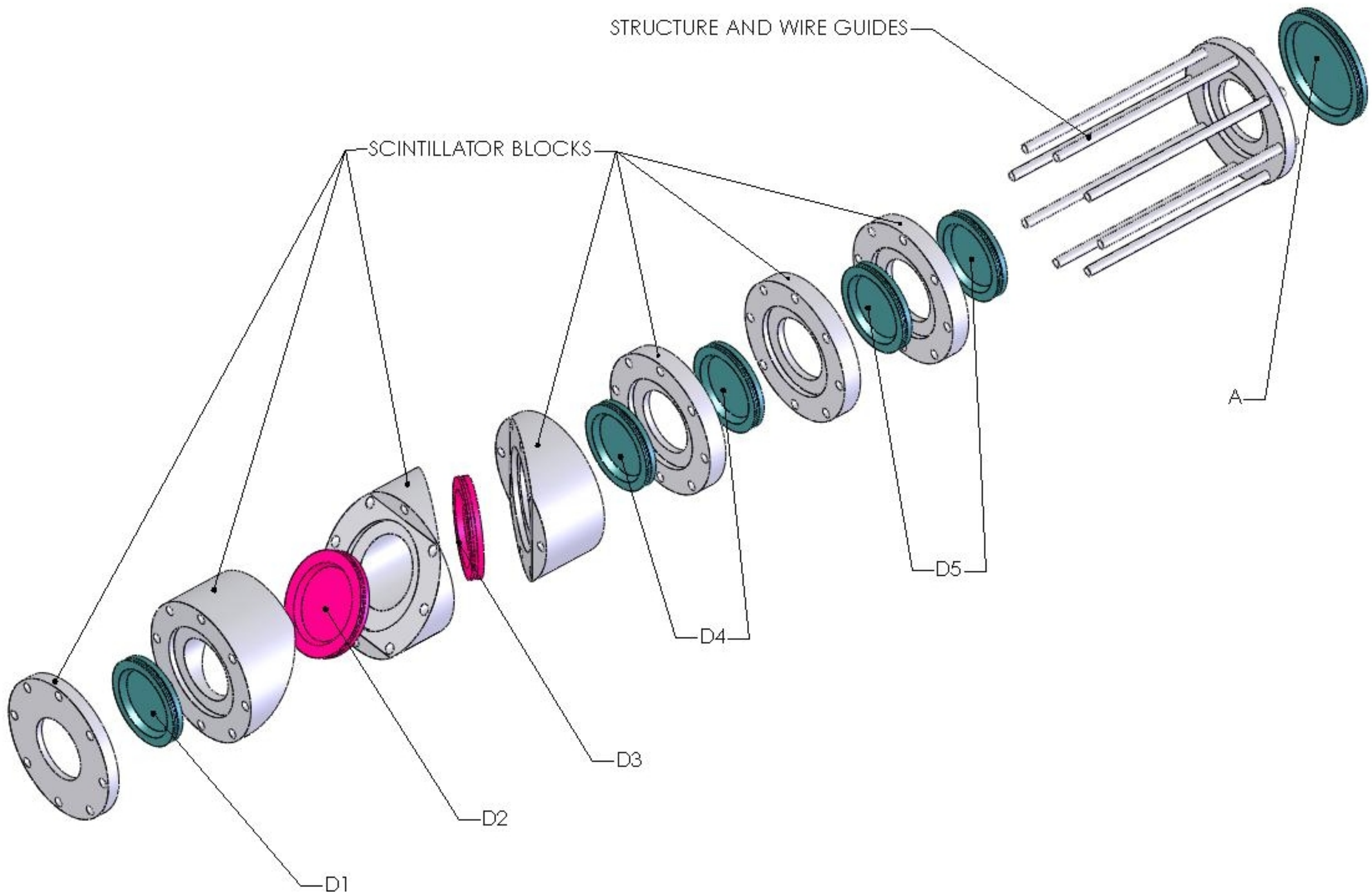
STRUCTURE AND WIRE GUIDES
SCINTILLATOR BLOCKS
A
D5
D4
D3
D2
D1

Ring ADIS

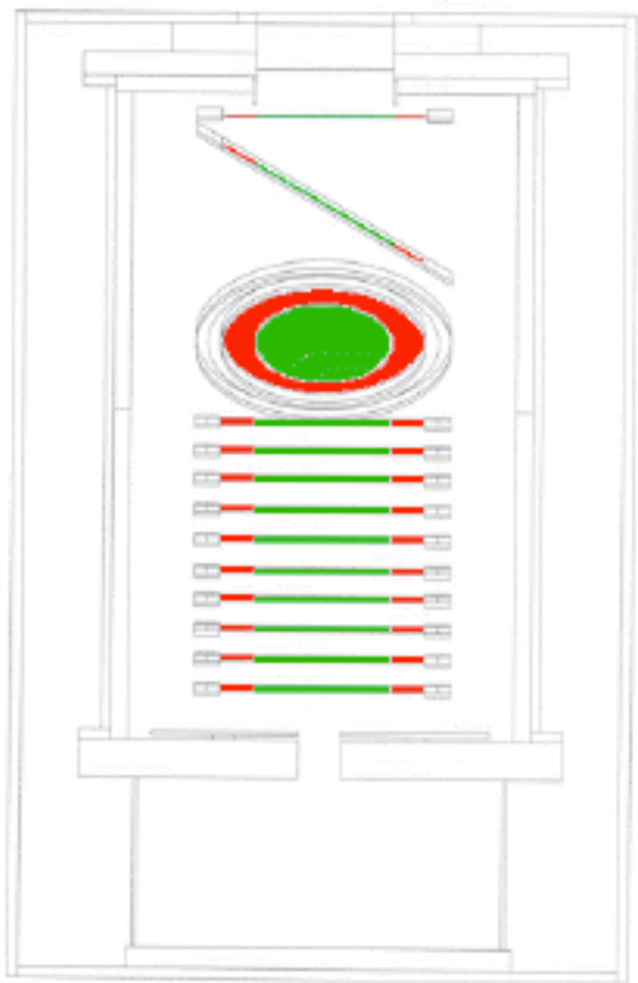

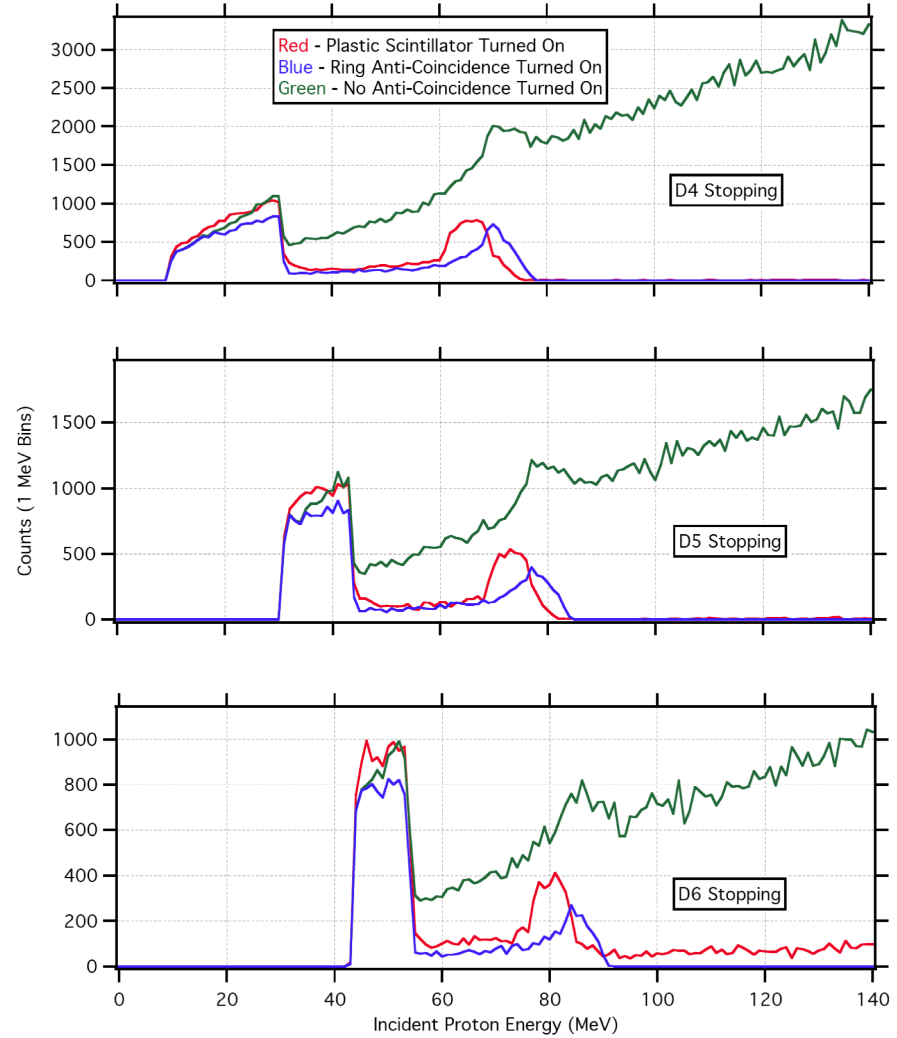

Undergraduate: Eddie LaVilla

Reduce Mass

EHIS significantly more massive than required for many application.

Very conservative electronics

Use of “ring” anti-coincidence

Save ~50% mass

Closer detector spacing

improves geometrical factors

Table 2: Geometrical factors in cm2-sr for EHIS and ring EHIS			
	EHIS	**Ring ADIS**	**Ratio**
D4 stopping	1.18	4.16	353%
D5 stopping	0.86	3.1	360%
D6 stopping	0.49	2.06	420%

NOAA Announcement on Future of GOES

- Studies for next generation
- ~$1M for 6 (+1) month studies

I am leading UNH/SwRI on SW instruments

- Four particle telescopes
  - Ring-ADIS for new EHIS
- Magnetometer

Roy Torbert is leading on looking at S/C options

Due 7 November

Radioactive Dating of Cosmic Rays

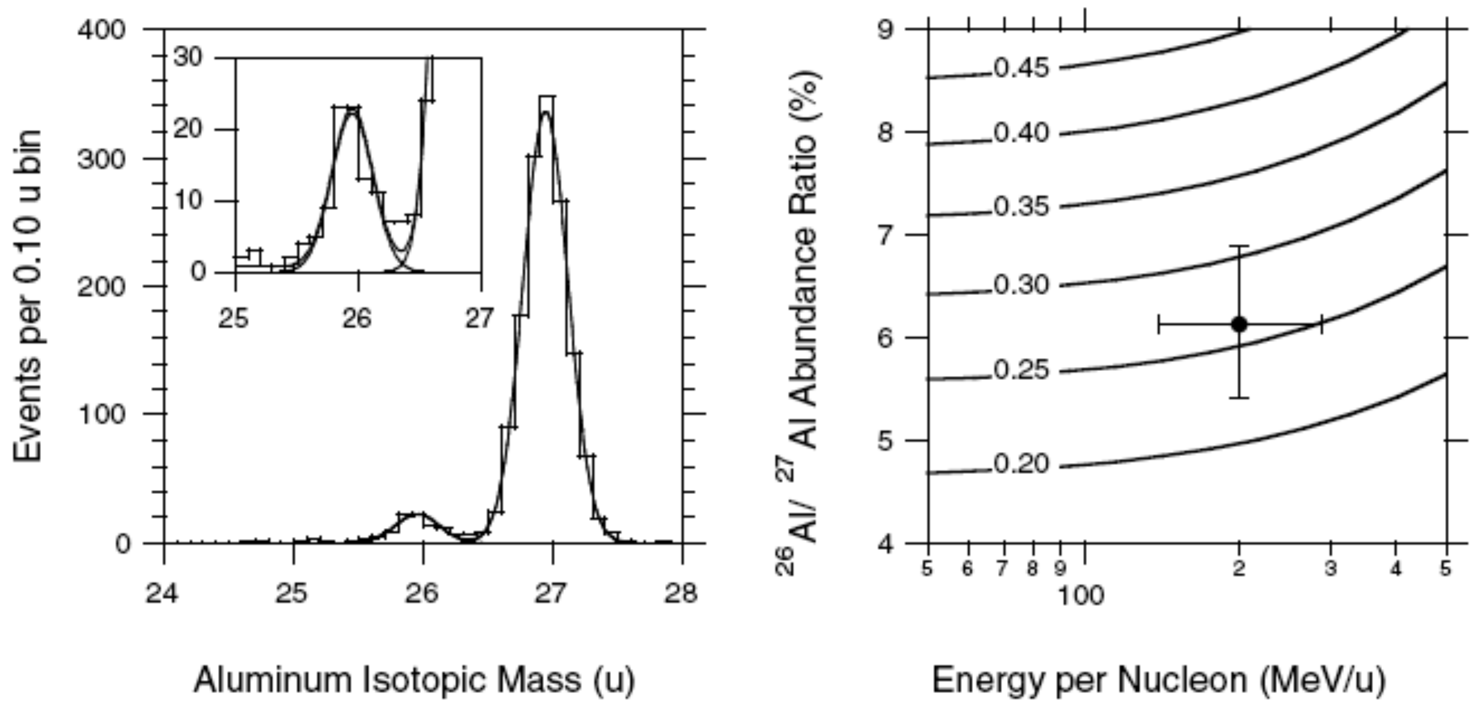

.

Figure 3. Left panel, *Ulysses* HET Mass histogram for aluminum. Inset shows ^{27}Al peak on expanded scale. Right panel shows the results of model calculations for various ρ (curves labeled in atom/cm^3) and the HET measurement (Simpson and Connell, 1998)

TABLE II

Summary of *Ulysses* HET radio-chronometer measurements.

Radio nuclide	Half-life (kyr)	$\langle E \rangle$ (MeV u^{-1})	ISM Density (atom cm^{-3})	Confinement time (Myr)
^{10}Be	1600	97	0.19 ± 0.03	26^{+4}_{-5}
^{26}Al	870[a]	200	$0.26^{+0.05}_{-0.04}$	19 ± 3
^{36}Cl	301	238	$0.28^{0.12}_{-0.10}$	10^{10}_{-6}
^{54}Mn	630[b]	238	$0.40^{+0.23}_{-0.15}$	$\sim$11

[a] β^+ partial half-life.
[b] β^- partial half-life $= 630 \pm 130$ (stat.) ± 110 (sys.) kyr (Wuosmaa *et al.*, 1998).

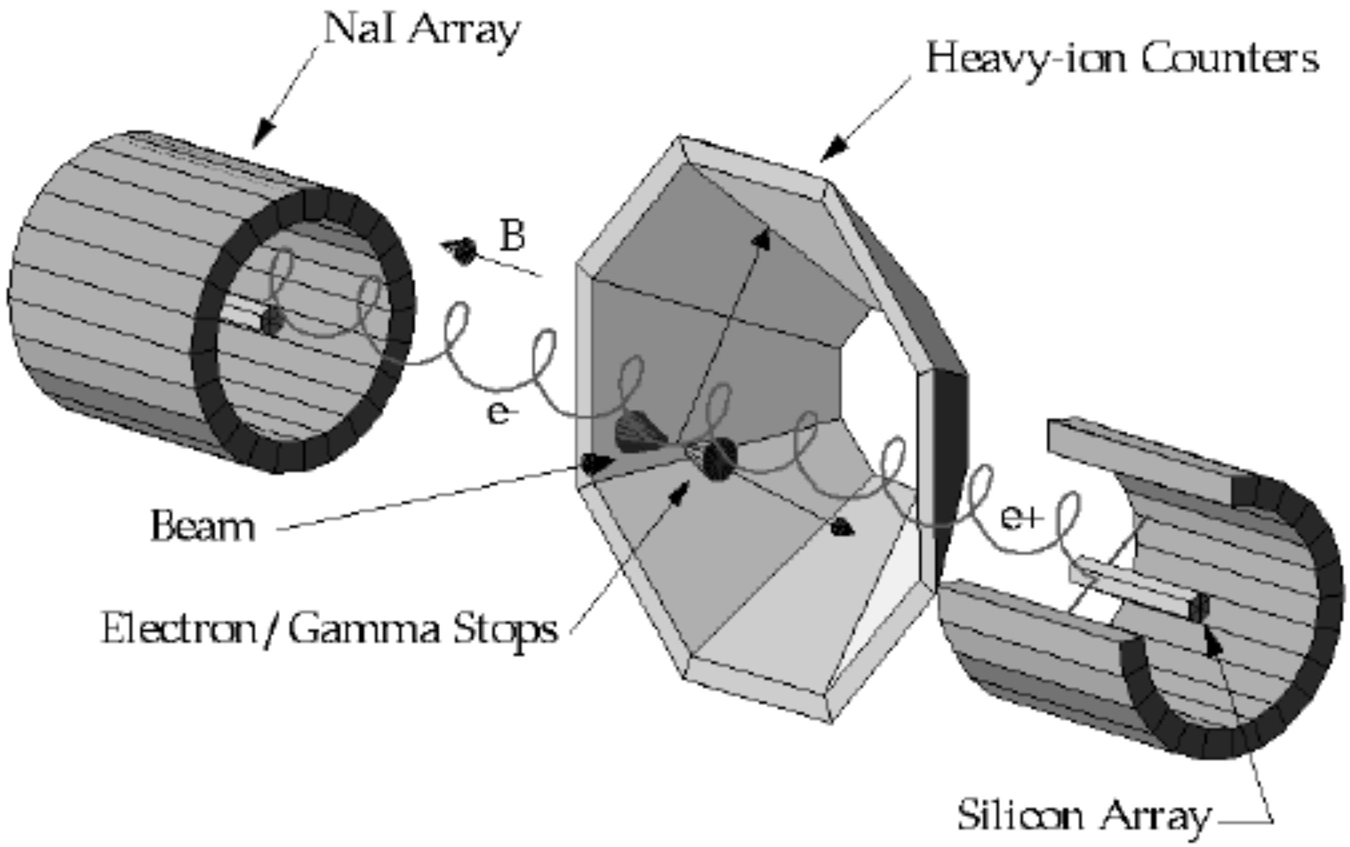
NaI Array
Heavy-ion Counters
B
e-
e+
Beam
Electron / Gamma Stops
Silicon Array

β^+ Decay Partial Half-Life of ^{54}Mn and Cosmic Ray Chronometry

A. H. Wuosmaa, I. Ahmad, S. M. Fischer, J. P. Greene, G. Hackman, V. Nanal, G. Savard, J. P. Schiffer, and P. Wilt
Physics Division, Argonne National Laboratory, Argonne, Illinois 60439

Sam M. Austin and B. A. Brown
National Superconducting Cyclotron Laboratory and Department of Physics and Astronomy, Michigan State University, East Lansing, Michigan 48824

S. J. Freedman
Lawrence Berkeley National Laboratory and Department of Physics, University of California, Berkeley, California 94720

J. J. Connell
Enrico Fermi Institute, University of Chicago, Chicago, Illinois 60637
(Received 25 September 1997)

The weak β^+ decay of the astrophysically significant radioisotope ^{54}Mn has been observed. The energies of positrons from a chemically purified ^{54}Mn source were measured using the APEX spectrometer at Argonne National Laboratory. We deduce a β^+ decay branch of $(1.20 \pm 0.26) \times 10^{-9}$, corresponding to a partial half-life of $(7.1 \pm 1.5) \times 10^8$ yr. The implications of this value for cosmic-ray confinement times are discussed in light of recent satellite measurements of the cosmic-ray abundance of ^{54}Mn. [S0031-9007(98)05458-1]

PACS numbers: 23.40.Hc, 26.40.+r, 27.40.+z, 98.38.−j

The radioisotope ^{54}Mn has attracted considerable interest over the past few years due to its importance as a potential chronometer for galactic cosmic rays (CRs) [1,2]. "Cosmic clocks," such as ^{10}Be or ^{26}Al, are long-lived radioisotopes present in Cosmic Rays, whose abundances, when measured in the solar system, are related to the time

erably higher than those suggested by astronomical methods [5]. A measurement of the even weaker β^+ decay to ^{54}Cr is experimentally more feasible due to the additional tag provided by the 511 keV positron annihilation radiation. Sur *et al.* [6] reported an upper limit on the β^+ branch of 4.4×10^{-8}, and da Cruz *et al.* improved

PICAP

Positron Identification by Coincident Annihilation Photons

Dan Tran’s Thesis Project

Modest energy ~2-8 MeV

Low mass (few kg)

Low power (few W)

No magnet

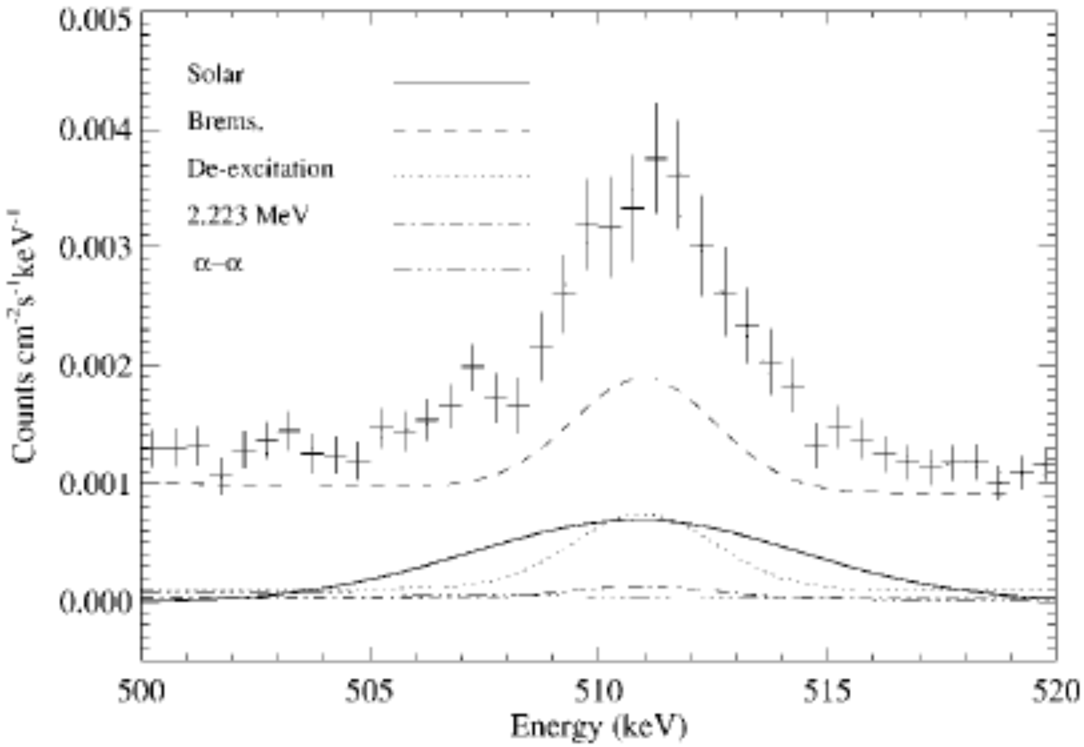

FIG. 2.—Fitted components of the 511 keV annihilation line observed during the time interval from 00:27:20 to 00:43:20 UT. The data points show the total background-corrected count spectrum and the best fit (*thin solid curve*). Instrumental contributions to the total line are plotted individually. The thick solid curve shows the Gaussian shape of the derived solar annihilation line.

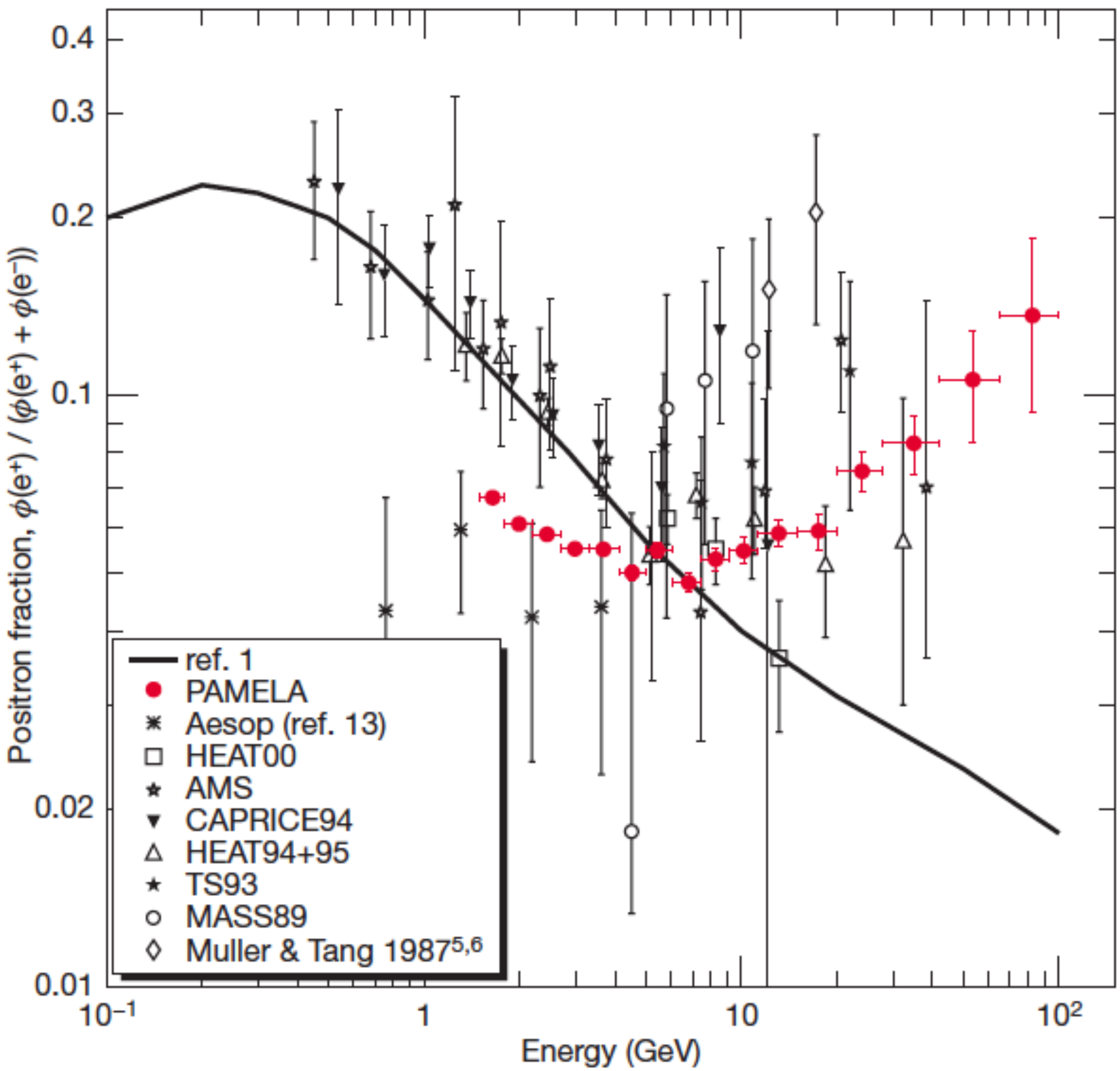

Positron fraction, $\phi(e^+) / (\phi(e^+) + \phi(e^-))$
0.4
0.3
0.2
0.1
0.02
0.01
10^{-1}
1
10
10^2
Energy (GeV)
ref. 1
PAMELA
Aesop (ref. 13)
HEAT00
AMS
CAPRICE94
HEAT94+95
TS93
MASS89
Muller & Tang 1987[5,6]

Charge sign effects in modulation of cosmic rays

Proton/electron ratio at same rigidity

Velocity effects

Prefer e^+/e^- ratio

Same energy

Same velocity

Same rigidity

Model of PICAP Detector Scheme

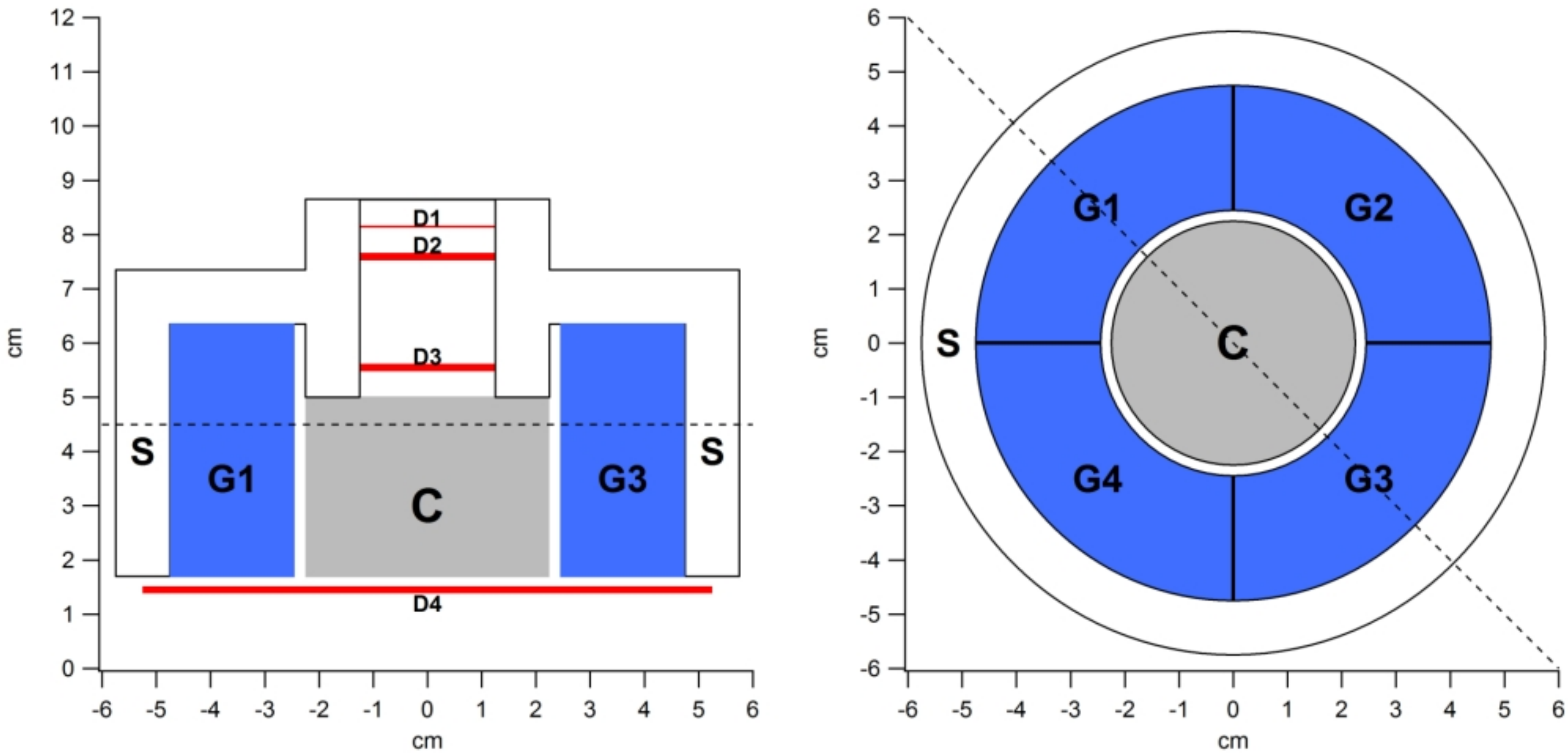

Prototype Design

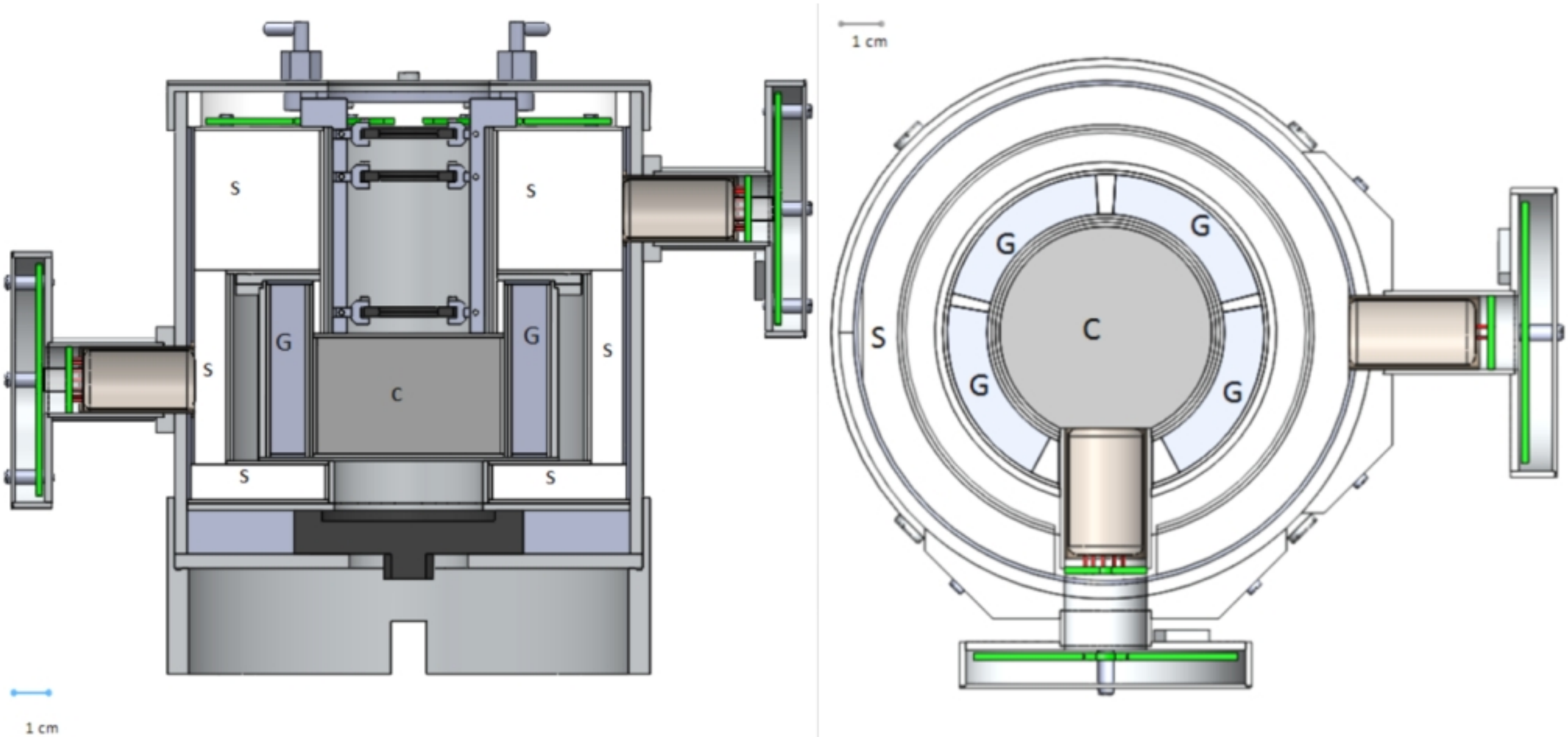

PICAP Prototype

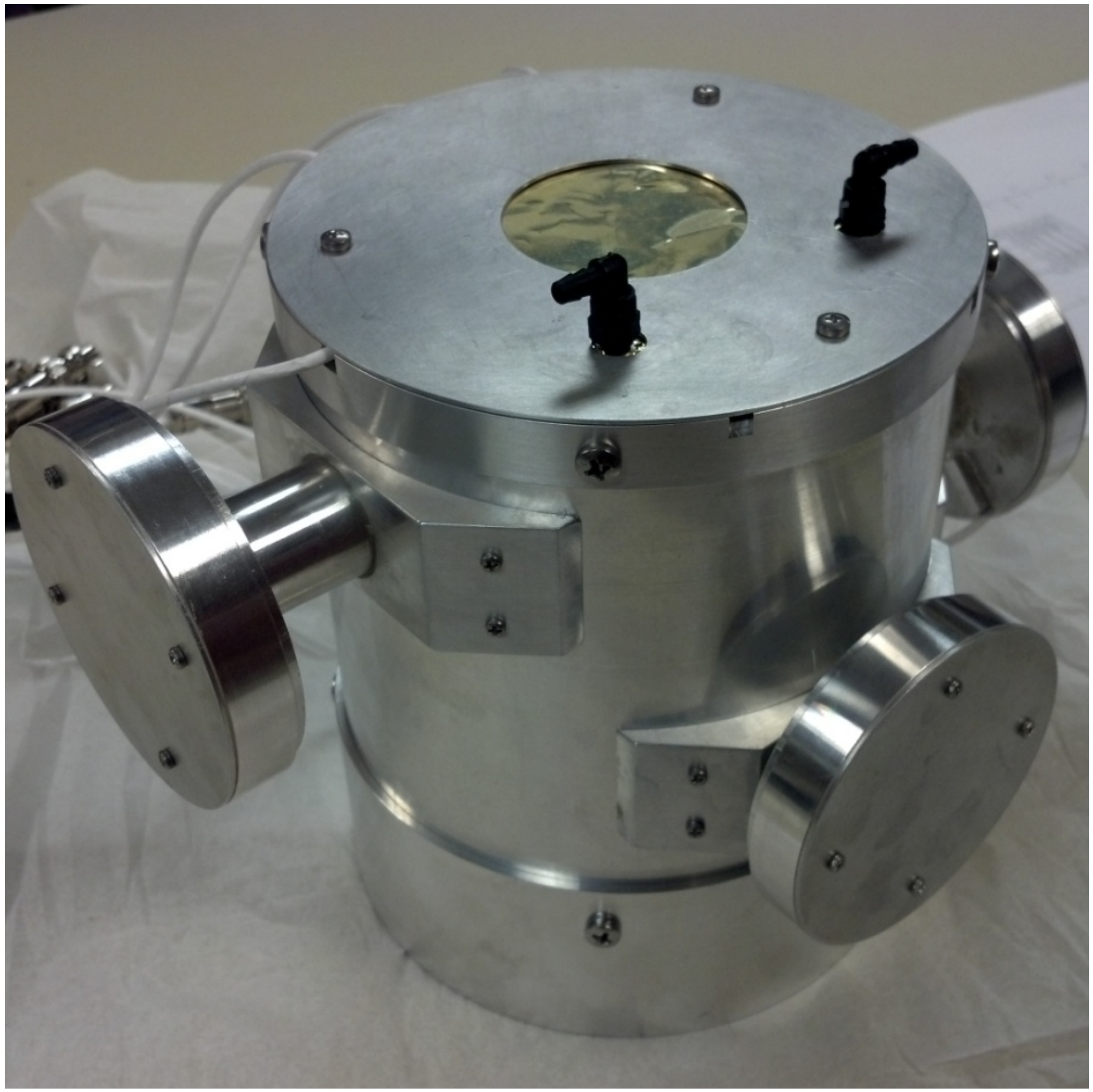

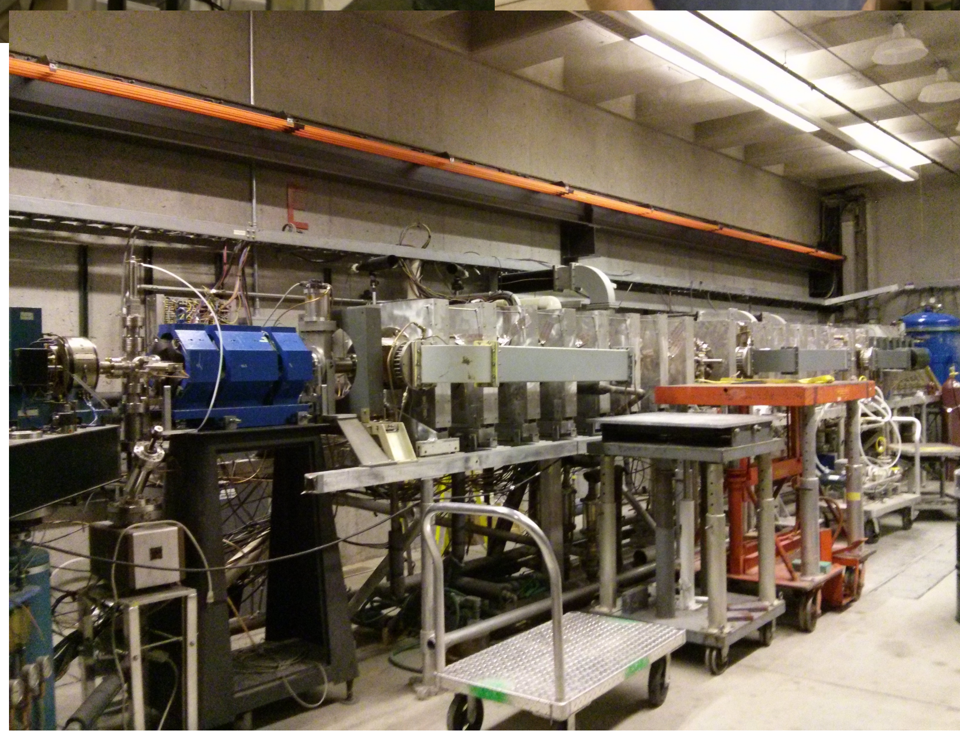

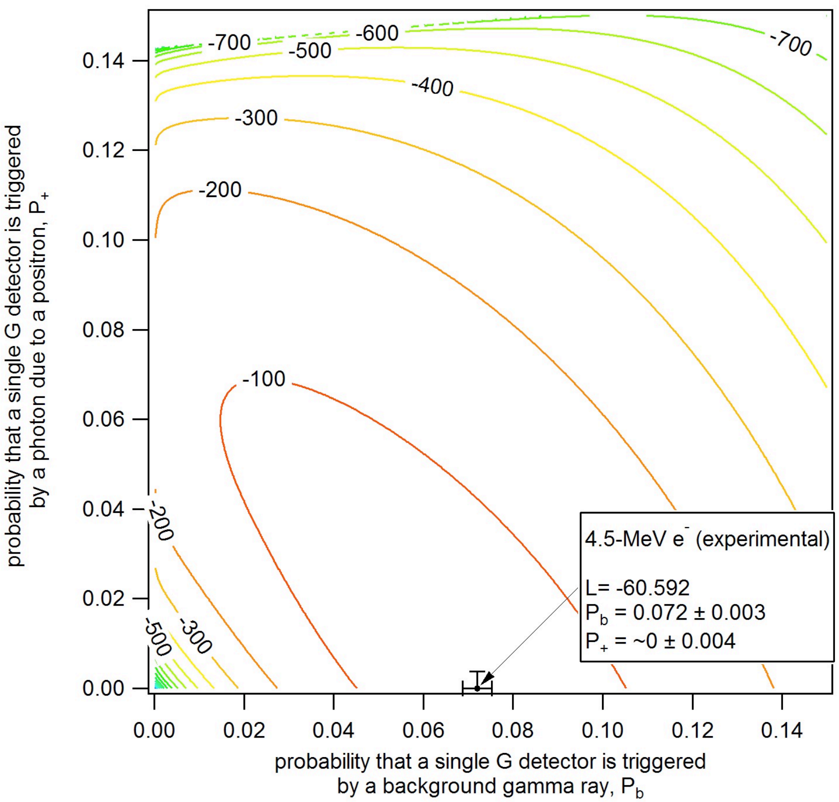
4.5-MeV e⁻ (experimental)
L= -60.592
P_b = 0.072 ± 0.003
P_+ = ~0 ± 0.004
-700
-600
-500
-400
-300
-200
-100
probability that a single G detector is triggered by a photon due to a positron, P_+
probability that a single G detector is triggered by a background gamma ray, P_b
0.00
0.02
0.04
0.06
0.08
0.10
0.12
0.14

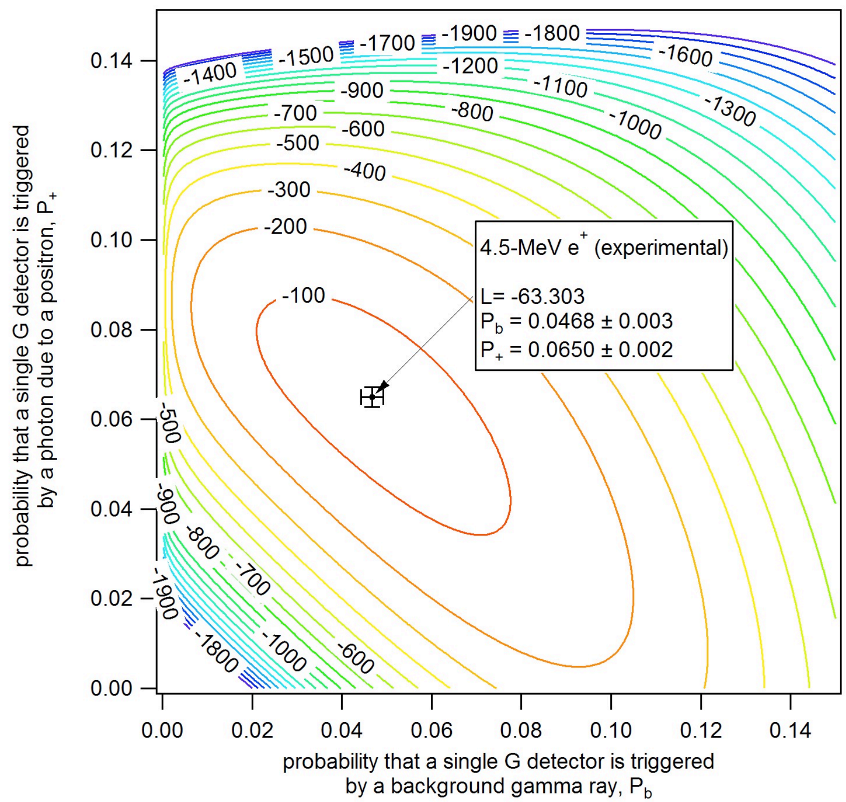
4.5-MeV e⁺ (experimental)
L= -63.303
P_b = 0.0468 ± 0.003
P_+ = 0.0650 ± 0.002
-1900
-1800
-1700
-1600
-1500
-1400
-1300
-1200
-1100
-1000
-900
-800
-700
-600
-500
-400
-300
-200
-100
probability that a single G detector is triggered by a photon due to a positron, P_+
probability that a single G detector is triggered by a background gamma ray, P_b
0.00
0.02
0.04
0.06
0.08
0.10
0.12
0.14

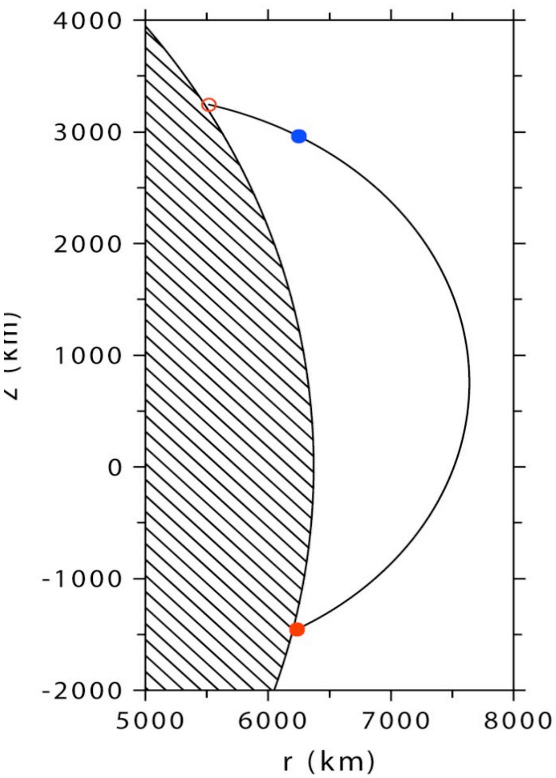

4000
3000
2000
1000
0
-1000
-2000
z (km)
5000
6000
7000
8000
r (km)

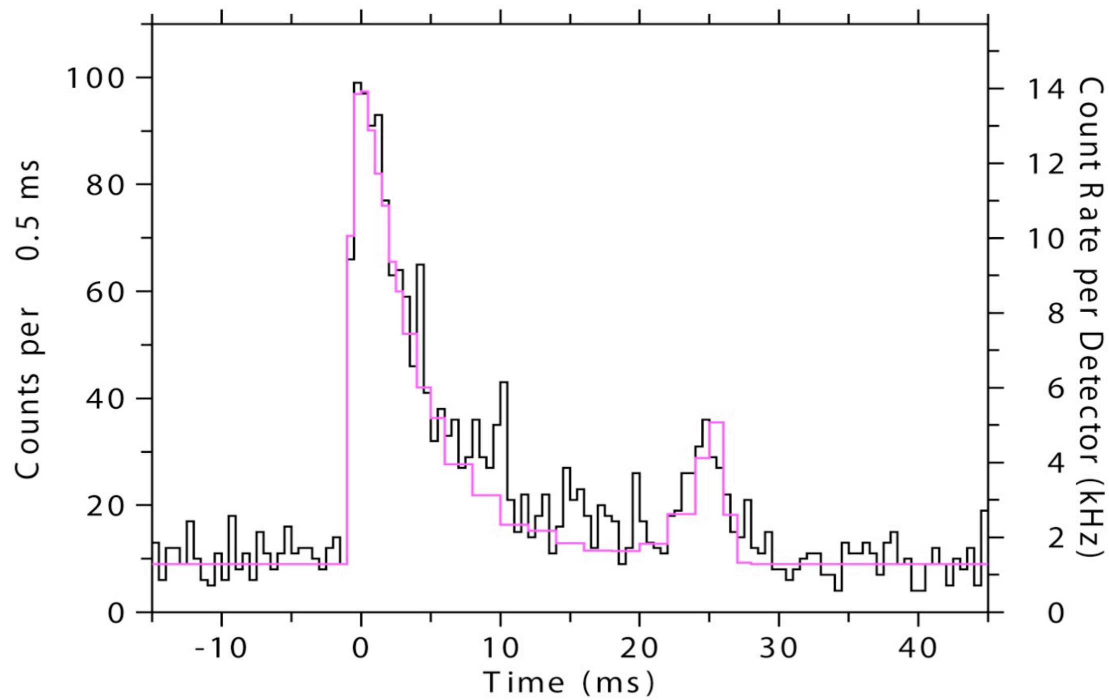

100
80
60
40
20
0
Counts per 0.5 ms
-10
0
10
20
30
40
Time (ms)
14
12
10
8
6
4
2
0
Count Rate per Detector (kHz)

THunderstorm Energetic Radiation MOnitor (THERMO)

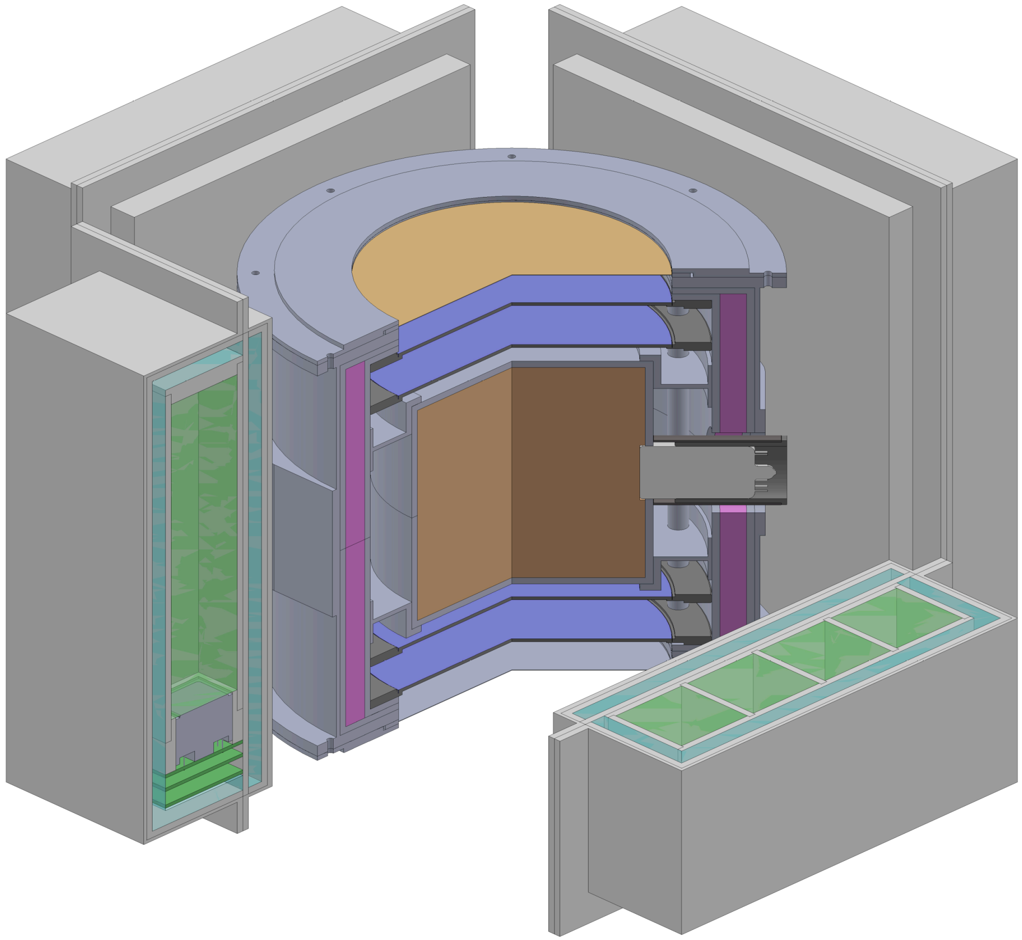

Joe Dryer, PI

Chemical Vapor Deposited (CVD) synthetic diamond

Cherenkov_radiation-animation.gif

Table 1. Cherenkov Radiators Characteristics				
	Synthetic Diamond	Lead-Fluoride	Synthetic Sapphire	Pilot-425 (Lucite)
Index of refraction	2.42	1.89	1.77	1.51
Density	3.52 g/cm^3	~7.7 g/cm^3	3.97 g/cm^3	1.18 g/cm^3
Proton Threshold	92 MeV	167 MeV	202 MeV	310 MeV
Electron Threshold	51 keV	91 keV	110 keV	175 keV
Residual Scintillation	< 3%		~20%	~5%

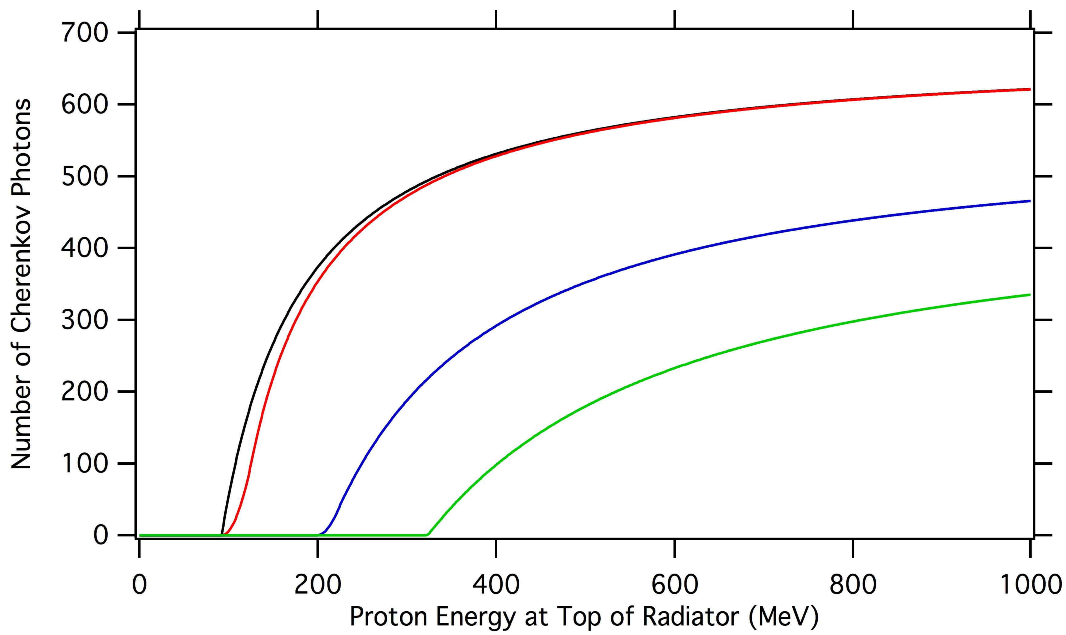

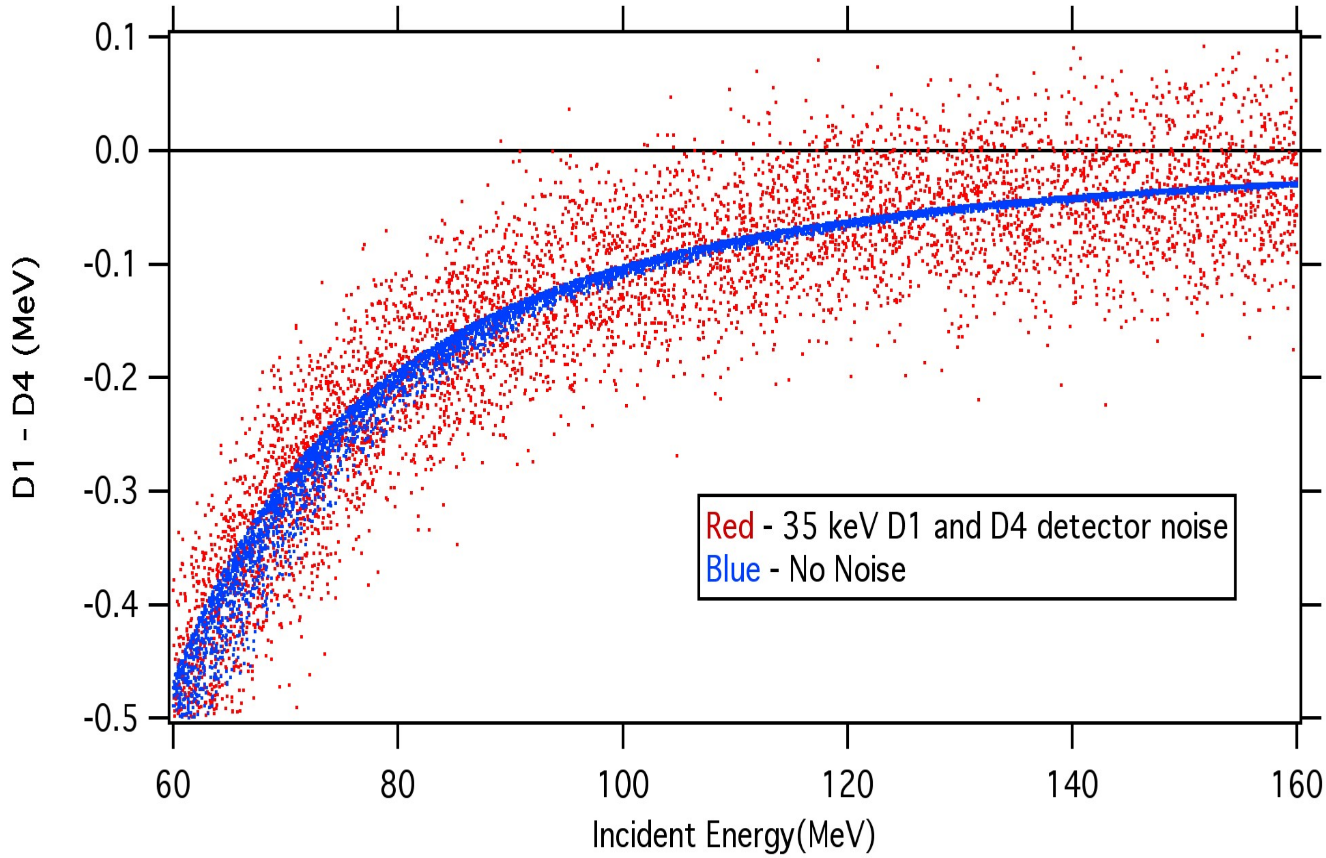

0.1
0.0
-0.1
-0.2
-0.3
-0.4
-0.5
D1 - D4 (MeV)
60
80
100
120
140
160
Incident Energy(MeV)
Red - 35 keV D1 and D4 detector noise
Blue - No Noise

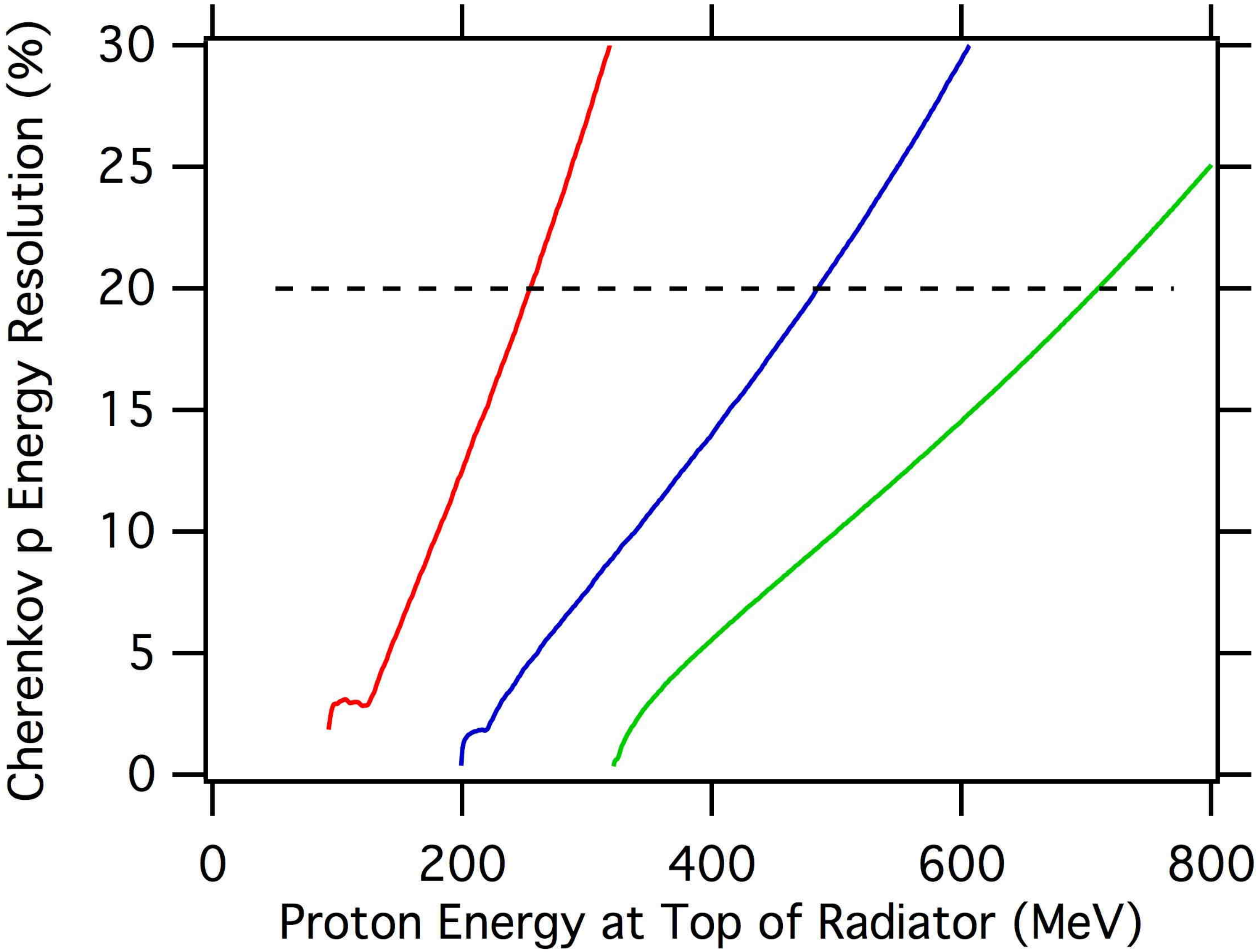

Cherenkov p Energy Resolution (%)
0
5
10
15
20
25
30
0
200
400
600
800
Proton Energy at Top of Radiator (MeV)

Spectra from the peak of the 29 September 1989 SEP event

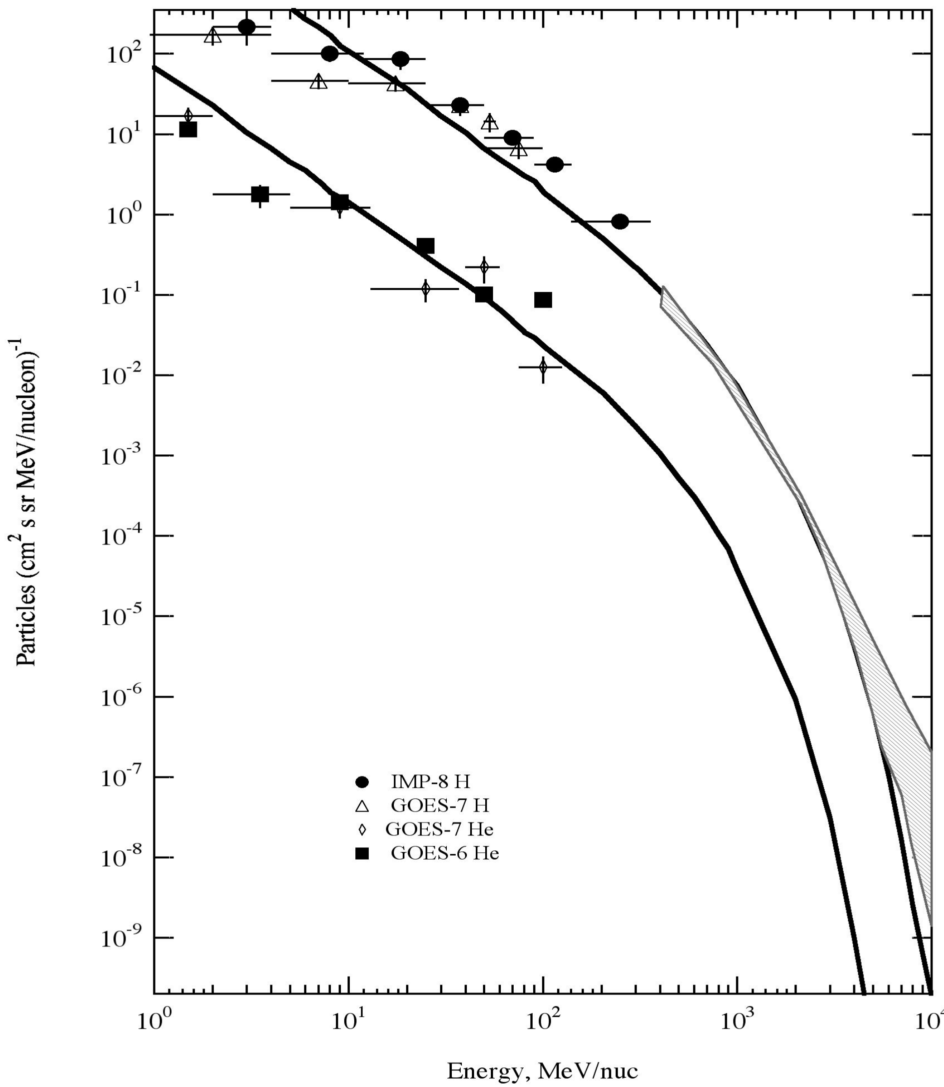

From: Lovell et al., JGR, 103, 23733, 1998
Fitted curves are of the form from Ellison and Ramaty, ApJ, 298, 400, 1985
Shaded area from neutron monitor data as per Lovell et al.

Nuclear Inst. and Methods in Physics Research, A 942 (2019) 162338

Contents lists available at ScienceDirect

Nuclear Inst. and Methods in Physics Research, A

journal homepage: www.elsevier.com/locate/nima

A novel synthetic diamond Cherenkov radiator for measuring space radiation

J.J. Connell [a,*], C. Lopate [a], J.W. Tabeling [b]

[a] Space Science Center, and Department of Physics and Astronomy, the University of New Hampshire, Durham, NH 03824, USA
[b] Applied Diamond, Inc., Wilmington, DE 19805, USA

ARTICLE INFO

Keywords:
Cosmic ray instruments
Solar energetic particle instruments
Cherenkov detectors
Spacecraft instruments
Diamond radiators

ABSTRACT

The measurement of cosmic rays and Solar energetic particles in space is basic to our understanding of the Galaxy, the Sun, phenomena in the Heliosphere and the emerging field of space weather. For these reasons, cosmic ray instruments are common on both scientific spacecraft and operational spacecraft such as weather satellites.

Cosmic rays (CRs) and Solar energetic particles (SEPs) include ions over the full range of elements found in the Solar System. High-resolution measurements of the energy spectra of space radiation are key to understanding both acceleration and propagation processes. An inherent challenge is the large range of energies of such spectra. Cosmic ray energies range up to over 10^{21} eV, while SEPs can reach a few GeV. Multi-instrument measurements are currently required to cover the full range of particle energies. Indeed, the highest energy particles, due to the rarity, can only be measured with ground-based instruments using the atmosphere as a calorimeter.

Some Major Threads

Space Science, astrophysics and space weather

Closely connected

Space physics has illuminated astrophysics

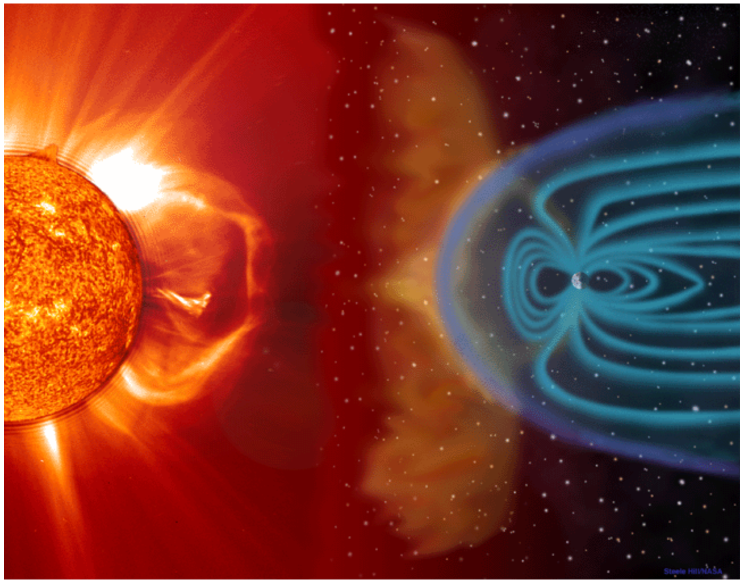

Space physics has illuminated astrophysics

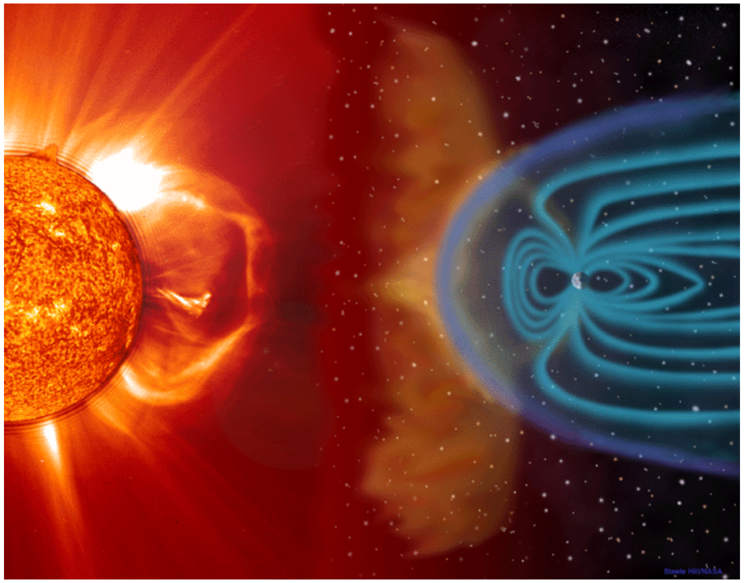

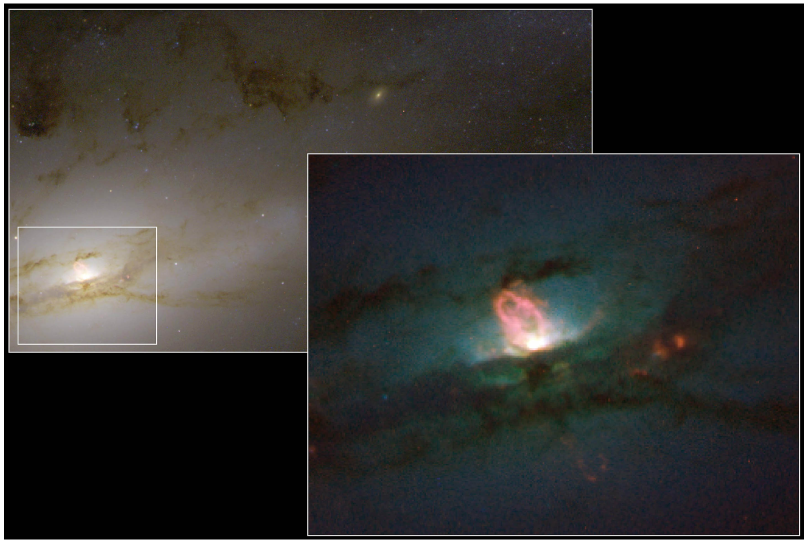

Astrophysics has illuminated space physics

Some Major Threads

Space Science, astrophysics and space weather

Closely connected

Developing space instruments is challenging

ADIS conceived about 1999

Funded for development 2002

EHIS project started 2004

GOES-R (-16) launch 2016

GOES-U launch 2023 (maybe!)

Energetic charged particles are ubiquitous